Innovative protection schemes through hardware-in-the-loop dynamic testing.

Feras Alasali [a], Naser El-Naily [b], Haytham Y. Mustafa [b], Hassen Loukil [c], Saad M. Saad [b], Abdelaziz Salah Saidi [d], William Holderbaum [e,*]

[a] *Department of Electrical Engineering, Faculty of Engineering, The Hashemite University, Zarqa 13133, Jordan*
[b] *Department of Electrical Engineering, College of Electrical and Electronics Technology, Benghazi 5213, Libya*
[c] *Department of Electrical Engineering, College of Engineering, King Khalid University, Abha 61413, Saudi Arabia*
[d] *Université de Tunis El Manar, École Nationale d'Ingénieurs de Tunis, Laboratoire des Systèmes Électriques, Tunisie*
[e] *School of Science, Engineering and Environment, University of Salford, Salford, UK*

ARTICLE INFO

ABSTRACT

In microgrid environments, the behaviour of Distributed Generation (DG) during fault conditions varies significantly based on DG types and penetration levels. Conventional Overcurrent Relays (OCRs) with standard time-current characteristics may exhibit limitations during excessive fault scenarios, leading to OCR operating delays and mis-coordination within the microgrid. This study proposes a novel constraint on the maximum Current Multiplier Setting (CMS) and utilizes Water Cycle Algorithm (WCA) and Particle Swarm Optimization (PSO) techniques to optimize the Time Multiplier Setting (TMS). Comparative dynamic analysis through real-time validation shows that the non-standard OCR approach outperforms the standard IEC scheme across all grid operation modes with different type, size and location of DGs. For instance, under F1 conditions, the tripping time of OCR1 was reduced from 0.0226 seconds (IEC) to 0.000981 seconds (non-standard). HIL results further affirm the efficacy of the proposed scheme. The optimization process, implemented in MATLAB and validated using ATP/EMTP simulations and SIPROTEC 7SJ62 relays, demonstrates enhanced microgrid protection coordination, improving system reliability and performance.

Abbreviations

DG	Distributed Generation
OCR	Overcurrent Relay
CMS	Current Multiplier Setting
WCA	Water Cycle Algorithm
PSO	Particle Swarm Optimization
PV	Photovoltaic

* Corresponding author at: University of Salford, Salford, UK.
E-mail addresses: ferasasali@hu.edu.jo (F. Alasali), naseralnaile222@gmail.com (N. El-Naily), almahmoudy@ceet.edu.ly (H.Y. Mustafa), hloukil@kku.edu.sa (H. Loukil), smuftah@ceet.edu.ly (S.M. Saad), saidiabdelaziz@yahoo.fr (A.S. Saidi), w.holderbaum@salford.ac.uk (W. Holderbaum).

IIRER	Inverter-Interfaced Renewable Energy Resources
EMT	Electromagnetic Transient
DOCR	Directional Overcurrent Relay
GA	Genetic algorithm
HIL	Hardware-in-the-Loop
ATP	Alternative Transient Program
TMS	Time Multiplier Settings
CTI	Coordination Time Interval
DN	Distribution Network
PS	Plug Setting
T	Total tripping time
$t_{j,k}$	Tripping time of the relay j at fault k
W	Likelihood of a fault occurring on a particular line
$t_{b,k}$	Tripping time of the backup relay during fault k
$t_{p,k}$	Tripping time of the primary relay during fault k
Isc	Short circuit current
Ip	Pickup current

1. Introduction

1.1. Background

DGs, particularly through Photovoltaic (PV) and wind energy systems, have gained traction globally as a sustainable solution to environmental concerns. The excessive integration and adoption of DGs, such as solar and wind power, has reshaped the energy landscape, driving a transition towards a more sustainable future. However, the integration of these resources into distribution networks introduces unknown challenges for protection engineers, necessitating a deeper understanding of their dynamic behaviour during fault conditions [1]. The integration of these resources into distribution networks, facilitated by power electronic converters, presents a transition in power system dynamics. However, this integration also includes unusual challenges for protection engineers, particularly in understanding the dynamic response of Inverter-Interfaced Renewable Energy Resources (IIRERs) during faults. Compared to conventional energy sources, IIRERs respond differently during faults, as their unique control architectures govern their behaviour. This unpredictability and inconsistency in response increases the challenges for protection engineers, as conventional short-circuit software may not adequately analyze the dynamic inverter control response within the protection time frame [2].

Electromagnetic Transient (EMT) simulation is critical for analyzing the interaction between inverters and the power grid, especially for assessing control stability, fault impacts, and post-fault dynamics [3,4]. This study highlights the necessity of EMT simulation in ensuring grid reliability amidst increasing renewable energy penetration through HIL systems. EMT simulation provides detailed insights into control interactions, stability issues, and the impact of unbalanced faults, crucial for high-penetration scenarios of inverter-based resources [5]. Despite being computationally intensive, these simulations are essential for effective analysis, necessitating efficient modelling techniques [6]. As inverter-based renewable energy resources grow, EMT simulation becomes increasingly important for understanding control dynamics, fault impacts, and grid stability, ensuring reliable power grid operations [7–9].

1.2. Literature review

A reliable protection coordination scheme is vital for ensuring the maximum reliability of a power system. Effective protection during faults is essential to separate only the faulty sections while keeping the healthy parts of the feeder. Achieving an efficient protection scheme requires precise coordination between primary and backup relays, ensuring quick response to faults and proposer islanding of faulty sections [10,11]. Directional Overcurrent Relays (DOCRs) have emerged as fundamental relaying devices due to their cost-effectiveness and efficient operation. The transition from electromechanical to numerical-based relays has revolutionized protection systems, offering enhanced flexibility, robustness, and adaptability to modern power grid requirements [12]. In general, various practical strategies have been explored for relay coordination, including plug setting, time multiplier setting, and user-defined characteristics, to optimize protection schemes in the context of increasing DG penetration and bidirectional current flow. Additionally, advancements in relay technology have paved the way for the development of smart grids, resilient to the challenges posed by DG integration [13].

The integration of user-defined relay curves offers a flexible approach to relay coordination, enabling suitable protection solutions to meet evolving system demands [14,15]. Efficient protection schemes facilitate the rapid disconnection of faulty sections, protecting the overall stability and reliability of the power network. Effective coordination between primary and backup relays is essential and critical to prevent unnecessary tripping of larger network sections during fault [16]. The evolution that happened from electromechanical to numerical-based relays has revolutionized protection systems, offering enhanced reliability, flexibility, and adaptability to modern grid requirements. Numerical relays provide features such as fault recorder data storage, adaptive relaying, and immunity to component parameter variations [17]. Flexible settings approaches and user-defined relay curves offer optimized protection solutions, allowing for flexible relay characteristics based on system conditions [12,18]. The Commercial numerical relays offer options for selecting relay operating characteristics, empowering engineers to customize protection solutions according to specific system

requirements [19]. The power systems continue to evolve and integrate increasing levels of distributed generation, and reliable protection coordination remains crucial. The transition to numerical-based relays and the integration of user-defined characteristics offers profitable routes for optimizing protection schemes and ensuring grid resilience in the complexion of changing system dynamics [20,21–24]. Table 1 highlights the research gaps in modern OCR schemes. These include the lack of comprehensive simulation analyses across various scenarios, insufficient exploration of OCR schemes' performance under different grid operating modes, a lack of focus on diverse network configurations such as micro-grids, scarcity of studies conducting real hardware tests to validate OCR schemes, and inadequate consideration of industrial limitations and practical constraints in implementing these schemes. The literature review highlights several innovative techniques proposed for power system protection, each addressing specific challenges and aiming for improved efficiency and reliability. However, despite these advancements, there needs to be more literature regarding validating these techniques through experimental verification. While the proposed methods in Table 1 show promise theoretically, their practical effectiveness remains to be tested with experimental validation. This gap highlights the need for more comprehensive experimental validation to assess these innovative protection methods' real-world applicability and performance. Therefore, the results and verification in this study prioritize experimental validation to ensure the reliability and effectiveness of advanced protection methods in real-world power systems.

1.3. Contributions

This research introduces an innovative approach to address the challenges raised by excessive fault currents resulting from DG interconnection, particularly in microgrid environments. A novel non-standard characteristic is proposed, taking into account the maximum Current Multiplier Setting (CMS) of industrial relays to enhance compliance with heightened fault currents. These non-standard characteristics, easily programmable in numerical relays from various manufacturers, offer adaptability and versatility. By employing the WCA and PSO, this study optimizes these non-standard characteristics to uphold the security, selectivity, and reliability of OCR schemes in microgrids, notably in islanded mode and low-fault current scenarios. Furthermore, this research employs user-defined characteristics programmed in relay software, such as DIGSI4 for feeder manager relays (SIPROTEC 7SJ62), extending the CMS to effectively handle excessive fault currents resulting from DG interconnection. Aiming to contribute towards filling this gap, this study highlights the following contributions:

- Proposal of a modern non-standard characteristic that considers industrial relays' maximum CMS to address excessive fault currents due to DG interconnection. Introduction of easily adjustable and reprogrammable non-standard characteristics for OCRs, applicable to numerical relays from various manufacturers.
- Comparative dynamic analysis through real-time validation between the new constraint and non-standard characteristics with conventional IEC standard characteristics in existing industrial relays installed in distribution networks.

Table 1
Summary of modern OCR schemes for power grids with DGs.

Ref	year	Characteristic curve type		simulation and analysis		DG	Optimization algorithms	Different network configurations	Hardware-in-the-loop (HIL)	Industrial Limitation
		standard	non-standard	Phasor RMS	EMTP					
[25]	2008	✓	✓	✓	×	×	Karush–Kuhn–Tucker	×	×	×
[26]	2015	✓	×	✓	×	✓	nonlinear programs	✓	✓	×
[27]	2017	✓	✓	✓	×	✓	×	✓	×	×
[28]	2018	✓	✓	✓	×	✓	Genetic algorithm (GA)	✓	×	✓
[29]	2018	✓	✓	✓	×	✓	GA	✓	✓	×
[30]	2020	✓	×	✓	×	×	Firefly Algorithm	×	×	×
[31]	2020	✓	×	✓	×	×	GA	×	×	×
[32]	2020	✓	✓	✓	×	✓	GA; Seeker algorithms; PSO	✓	×	×
[33]	2020	✓	✓	✓	×	✓	Differential Evolutionary	✓	×	×
[34]	2021	✓	✓	✓	×	✓	GA; PSO	✓	×	×
[35]	2021	✓	✓	✓	×	✓	GA; PSO	✓	×	×
[36]	2021	✓	×	✓	✓	✓	×	✓	✓	×
[37]	2021	✓	✓	✓	✓	✓	×	✓	✓	×
[38]	2022	✓	✓	✓	×	✓	×	✓	×	×
[39]	2022	✓	×	✓	×	✓	GA	✓	×	×
[40]	2023	✓	×	✓	×	✓	Interior Point Simulated Annealing	✓	×	×
[41]	2023	✓	×	✓	×	✓	×	✓	×	×
[42]	2023	✓	✓	✓	×	✓	Hybrid GA-NLP algorithm	✓	×	×
[43]	2024	✓	✓	✓	×	✓	Nonlinear Program	✓	×	×
	Proposed approach	✓	✓	✓	✓	✓	PSO; WCA	✓	✓	✓

- Integration of Hardware-in-the-Loop (HIL) testing methodology to validate the proposed optimization techniques and non-standard characteristics in real-time scenarios. Real-time validation of results using OMICRON-256 on SIPROTEC 7SJ62 Multi-function Protection Relay, affirming the efficacy of the proposed WCA in safeguarding microgrids against three-phase faults. Implementation of the optimization process was conducted using MATLAB, and short-circuit currents were simulated by Alternative Transient Program (ATP/EMTP) software, with validation using computerized test sets and Multifunction feeder manager relays (SIPROTEC 7SJ62).

In this study, the WCA and PSO were employed to tackle the coordination issue of the OCR schemes within the IEC benchmark grid. Specifically, a setting for nine OCRs was devised by optimizing Time Multiplier Settings (TMS) for each OCR within the IEEE 9-bus system, both with and without PVs. This optimization procedure was executed using MATLAB. Furthermore, the simulation of short-circuit currents was performed utilizing the ATP/EMTP software. The obtained short-circuit current signals are then inserted into a computerized test set (e.g. OMICRON-356) which is injected in analogue form to the Multifunction feeder manager relay (SIPROTEC 7SJ62) to validate its performance. The outcomes of the proposed WCA are contrasted with PSO. The efficacy and robustness of the suggested methodologies are evaluated using the IEEE 9-bus system simulated in ATP/EMTP. Real-time validation for the results is verified using OMICRON-256 on SIPROTEC 7SJ62 Multi-function Protection Relay. The proposed WCA affords efficient protection against three-phase faults in the grid. The objective function was formed to minimize the overall operational time while ensuring optimal coordination time intervals between the primary and backup relays. The objective function is maintained by maintaining appropriate Coordination Time Interval (CTI) to guarantee optimal grid operation when connected to PVs.
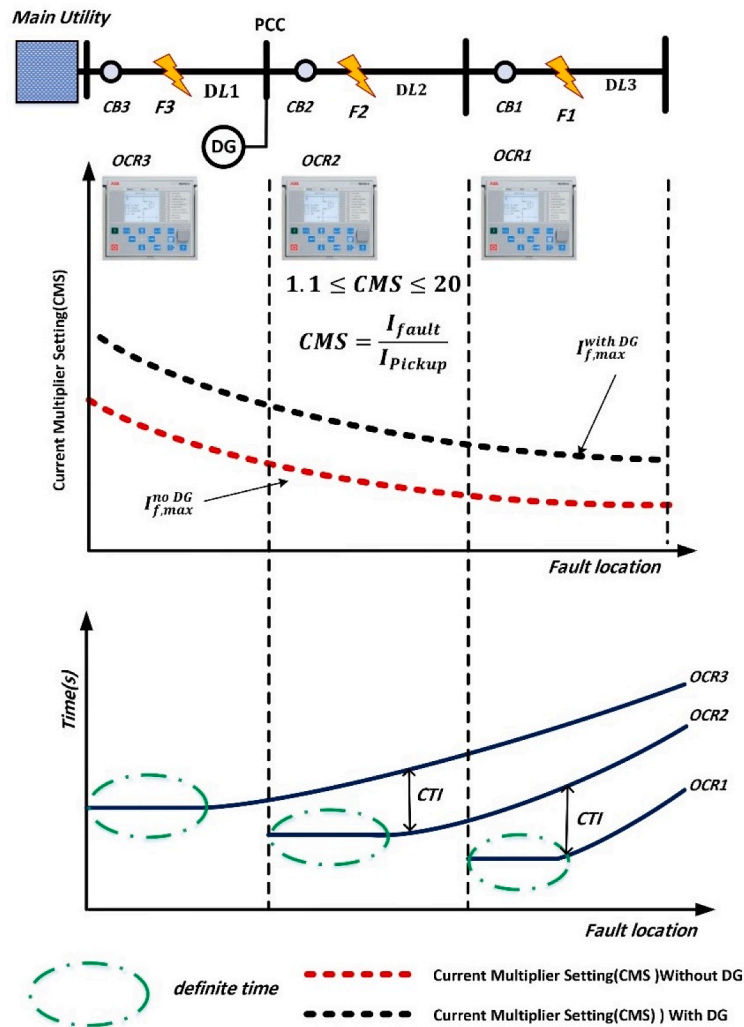

$$CMS = \frac{I_{fault}}{I_{Pickup}}$$

$$1.1 \le CMS \le 20$$

Fig. 1. Coordination of OCR Scheme in DN.

1.4. Outline of paper

This article is structured as follows: Section 2 introduces the problem description for the demonstration of DGs' impact on OCRs sensitivity. Sections 3 and 4 outline the methodology behind the proposed OCR protection schemes. Section 5 presents the discussion and analysis of simulation and HIL results. Finally, Section 6 concludes the article and provides insights into potential future research directions.

2. Problem description: demonstration of DG impact on OCR sensitivity

Microgrids provide efficient and economical generation sources, improving grid efficiency and resilience to main source failures. However, the continuous integration of DG in microgrids has led to more complex arrangements in DNs. Short-circuit currents within power grids exhibit notable variability owing to the penetration level of DGs and the intermittent nature of renewable energy-based DGs. The placement and magnitude of DG installations can reduce the influence of the upstream grid on fault currents within the downstream grid, thereby influencing the coordination of OCRs. As the penetration of DG units continues in the DN, fault current levels escalate, potentially surpassing the maximum current multiplication setting of tripping characteristics in industrial OCRs. This escalation could compromise the selectivity and sensitivity of the protection scheme when fault current levels exceed the OCR's tripping characteristics. This transition of DN to microgrids, with their complex arrangements and integration of DG, poses challenges for adequately planning and configuring protection schemes. The traditional OCR scheme, which relies on current measurement, might not be suitable for fault detection in various grid operation modes. The excessive fault currents encountered due to DG interconnection can affect the coordination of over-current protection schemes in DN. The characteristics and limitations of industrial relays, such as the maximum CMS and TMS, must be considered when coordinating over-current protection schemes.

2.1. Traditional coordination of OCR scheme in DN

OCRs are widely used to protect DNs systems. These devices operate based on a set of characteristics that define their response time as a function of the current flowing through them. The most common of these characteristics is the Inverse Characteristics (standard scheme), designed to trip faster as the current increases, as illustrated in Fig. 1. In this standard OCR protection scheme, the curve will be limited to CMS less than 20, where the CMS is the ratio between the fault and pickup currents. In the case of CMS more than 20, the standard OCR scheme will work in a definite time region. This can increase the miss-coordination events, having instantaneous tipping time without any time delay or high defined time for coordination.

In addition, integrating distributed generation (DG) into the network can lead to higher fault currents than CMS equal to 20. This is because DG units denoted in Fig. 1, such as solar panels or wind turbines, contribute additional current to the system during faults F1, F2, and F3, respectively. The influence of these high fault currents on the conventional current characteristics is significant. When the fault current is excessively increased, it can cause the OCR to trip instantaneously, regardless of the time delay set by the current characteristics. This can lead to a loss of selectivity in the protection scheme, as the OCR may trip before other protective devices closer to the fault. As shown in Fig. 2, Coordinating over-current protection schemes is crucial for ensuring the selectivity and reliability of protective relays in the DN. In the case of fault F1 in a microgrid, downstream faults exceeded the pickup current of OCRs installed in the network. The primary and backup over-current relay operation times OCR1 and OCR2, respectively, can be delayed due to the variations and exceeding in each relay's CMS. The overcurrent relays OCR2 and OCR3 could experience the same issue as in the case of faults F2 and F3 in the presence of DG. For that, new and more adaptive OCR characteristics of manufacturer OCRs should be considered when planning and applying OCR schemes with excessive short-circuit levels in DN. In other words, the high fault current
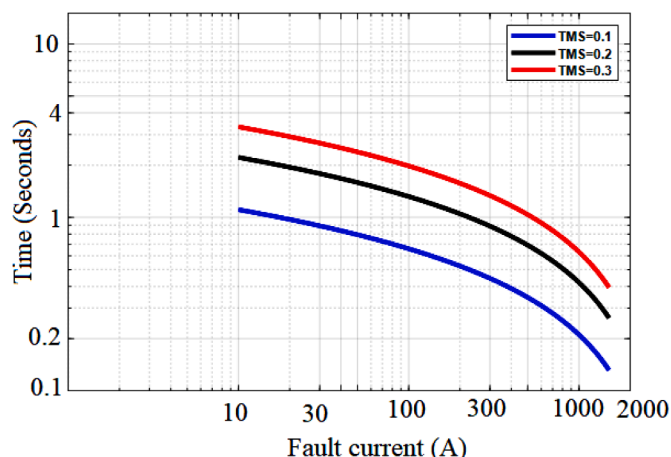

Fig. 2. A nonstandard tripping characteristic for TMS equal to 0.1, 0.2 and 0.3.

can affect the coordination between different OCRs in the system, making it difficult to isolate the faulty section without interrupting the power supply to other healthy grid parts. This is a significant technical challenge in modern power systems, especially with the increasing integration of DG. To address this issue, the paper proposes a non-standard tripping characteristic to enhance the performance of the OCR coordination scheme.

3. Optimal OCR coordination considering a modern CMS constraint

This paper presented a modern mathematical framework created to solve the problem of coordination between the OCR schemes within the restrictions and limitations of industrial relays. The introduced modern method adds a new constraint that considers the maximum current magnitude setting of the industrial relays used. This new improvement should enhance the efficiency of the optimization applied to the microgrid protection patterns.

3.1. Formulation of coordination problem

The most critical parameters for optimal coordination between OCRs that are in the DNs are the TMS and PS. These parameters control the time of operation of one protective relay to achieve critical coordination. PS, in particular, controlled the operation of OCRs. The TMS, as well as Plug Setting (PS), can reach an optimal value through WCA and PSO algorithms. Eq. (1) represents an optimization problem for the optimal coordination of OCR setting to achieve minimum tripping time [44,45].

$$T = \text{Min} \sum_{j=1}^{J} W \ t_{j,k} \tag{1}$$

where J is the number of OCRs, $t_{j,k}$ tripping time of the relay j at fault k, the weight W represents the likelihood of a fault occurring on a particular line. W is the weight that characterizes the tendency of failure to a line. For W =1, it means that the frequency of failure to any line should be equal. The cost function in Eq. (1) is solved under the following constraints [44,45].

- Coordination criteria:

Both the primary and backup OCRs detect the fault the moment it occurs at a specific point in the network. If the primary protection is unable to clear the fault within a predetermined period, the backup relay steps in to separate the fault by physically closing its contacts or circuit breakers. A Clearing Time Interval frames the CTI when the backup protection is allowed to act downstream while the fault happens. The CTI can be determined using the relay and the circuit breaker operating times. The coordination barriers and constraints can be illustrated using:

$$t_{b,k} - \ t_{p,k} \geq \text{CTI} \tag{2}$$

where $t_{b,k}$ is the tripping time of the backup relay during fault k. $t_{p,k}$ is s the tripping time of the primary relay during fault k. The Clearing Time Interval varies between 0.2 and 0.5 sec; CTI is 0.3 sec. in the considered work [44].

- OCRs operating time

Constraints on the operating time of OCRs present the need to ensure a minimum and maximum duration for relay operation are considered. This can be expressed as follows:

$$t_{j, \ min} \leq \ t_{j,k} \leq \ t_{j, \ max} \tag{3}$$

where $t_{j,min}$ and $t_{j,max}$ are the minimum and maximum tripping time of relay j, $0.001 \leq t_{j,k} \leq 4$

- TMS of each relay:

The Timing Multiplier Setting (TMS) plays a crucial role in fine-tuning the coordination of over-current relay operating times.

$$\text{TMS}_{j,min} \leq \ \text{TMS}_{j,k} \leq \ \text{TMS}_{j,max} \tag{4}$$

To ensure optimal coordination, the TMS values need to be within specific limits. Eq. (4) defines these limits as $\text{TMS}_{j,min}$ and $\text{TMS}_{j,max}$ are the minimum and maximum values of TMS of relay j, $0.01 \leq \text{TMS}_{j,k} \leq 3$

- Plug Setting (PS):

$$\text{PS}_{j,min} \leq \ \text{PS}_{j,k} \leq \ \text{PS}_{j,max} \tag{5}$$

where $PS_{j,min}$ and $PS_{j,max}$ are the minimum and maximum values of PS of relay j based on the load current, $100\% \leq PS_{j,k} \leq 120\%$. The ratio of the short circuit and pickup currents at the relay is the CMS.

- Current Multiplying Setting (CMS)

$$CMS_{j,min} \leq CMS_{j,k} \leq CMS_{j,max} \tag{6}$$

where $CMS_{j,min}$ and $CMS_{j,max}$ are the minimum and maximum values of CMS of relay j. In the Inverse Characteristics (standard scheme), $1.1 \leq CMS_{j,k} \leq 20$. The $CMS_{j,k} = \frac{IS_{j,k}}{IP_{j,k}}$, where the $IS_{j,k}$ and $IP_{j,k}$ are the short circuit and pickup currents at relay (j) and fault location (k). In this study, regarding the IEC standard, OCRs have normally inverse characteristics in (7) to determine the relay operating time.
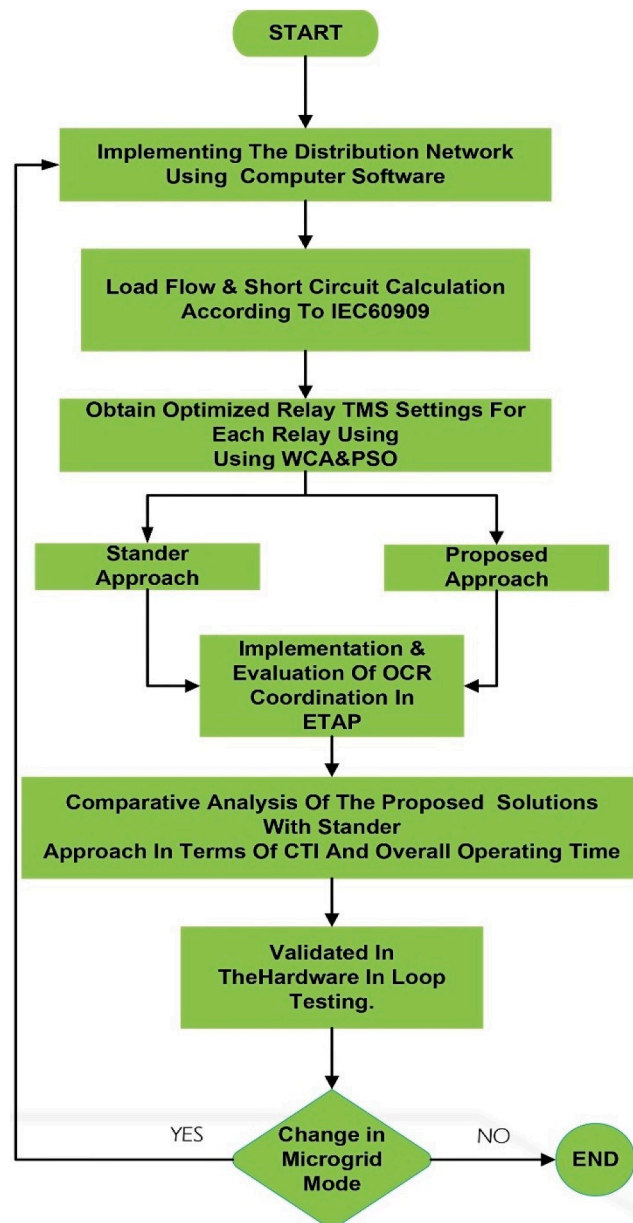

Fig. 3. General workflow of the OCRs coordination scheme.

7

$$t_{j,k} = \left(\frac{0.14 \ \text{TMS}_j}{\left(\ \text{CMS}_{j,k} \right)^{0.02} - 1} \right) \tag{7}$$

3.2. A nonstandard time–current characteristic

Fig. 2 illustrates how the nonstandard tripping feature, which decreases the tripping duration as the fault site gets closer to the source (maximum fault current), is dependent on the fault current value [46]. Furthermore, the intended nonstandard curve finds use in several fields, including the control of thermal stress in transformer and cable equipment. To ensure selectivity in OCRs coordination, the grading time must remain consistent and unaffected by the fault's location or level in the network. Eq. (8) introduces a novel nonstandard time-current characteristic for all relays, incorporating logarithmic and constant coefficients. This characteristic ensures that the grading time remains independent of fault level and location, thereby enhancing the selectivity of the protection system regardless of varying conditions. Unlike conventional inverse curves which may struggle to identify minor faults, the proposed nonstandard approach is particularly effective due to the influence of distributed generation sources on fault currents within the network. This innovative approach can significantly improve OCR coordination and minimize relay tripping time. Researchers have also utilized nonstandard characteristics for similar purposes, as demonstrated in previous studies [47,48]. The following equation, based on a logarithmic function, outlines the nonstandard tripping characteristic.

$$t_{j,k} = \left(a - b * \log_e \left(\frac{\text{IS}_{j,k}}{\text{IP}_{j,k}} \right) \right) * \text{TMS}_j \tag{8}$$

where a and b are constants equal to 5.8 and 1.35, as in [31]. The $\text{IS}_{j,k}$ and $\text{IP}_{j,k}$ are the short circuit and pickup currents at relay (j) and fault location (k). In this non-standard OCR protection scheme, the curve will be not limited to CMS less than 20 compared to the standard scheme. This can help to minimize the number of miss-coordination events, having instantaneous tipping time without time delay or high define time.

4. Proposed framework for optimal coordination of OCRs

Particularly when connecting to renewable energy recourses with variable energy feed, the microgrid's sensitivity to operating in various modes (connected and islanded mode) causes a significant shift in the number of fault currents. These factors reduce the sensitivity and dependability of microgrid protection schemes and complicate their operation. This study proposes and tests a new method for using contemporary numerical relay characteristics to coordinate all OCRs in substations, and process industries in microgrids. The non-standard characteristics that are now available in IEDs are effectively used in conjunction with software applications to shorten the time it takes to clear faults and prevent annoying tripping in the microgrid protection system.

The methods and structure of this study are outlined in Fig. 3. First, the standard DN (IEEE 9 bus) with and without PV systems are implanted by ETAP and ATP/EMTP simulations. Next, a load flow analysis utilizing the Newton-Raphson method is conducted to determine the current settings for each OCR and establish the initial relay settings. Subsequently, short-circuit calculations based on IEC 60909 (Sweeting, 2011) are conducted in different locations, both with and without PVs. Then, depending on the present levels of the different earth and phase faults, the ideal configuration for the OCR system was found using two optimization techniques (WCA and PSO). These robust optimization methods will be used to tackle the OCRS coordination challenges. These algorithms are initially implemented as computer software in the MATLAB environment in this study. Then, using ETAP industrial software, the effectiveness of the configuration acquired on the network protection system was confirmed. The suggested method guarantees the best OCR scheme configuration among all variations in the network's operating circumstances, resulting in the minimum tripping time. Finally, the results and relay configurations are tested and validated by using the Hardware in the loop testing.

4.1. Optimization algorithms

4.1.1. Water cycle optimization algorithm

Inspired by the natural water cycle, the WCA is a heuristic optimization approach [49]. Its effectiveness as a powerful optimization solution, implementable via the Optimization Toolbox in MATLAB/SIMULINK [50], has been shown in earlier power engineering research. To reduce the overall operation time, WCA is used in this study to address the coordination issue between OCRs as described in the previous sections. The primary process of WCA involves iterative steps:

1. Initial Parameters: A range of values are tested, and the best-performing ones are chosen to find the ideal value for each parameter.
2. Random Generation of Solutions: At the start of the process, a population of solutions is produced at random for the OCR coordination issue. The initial population can be represented as:

$$\text{TMS} = \left\{ \ \text{TMS}_1, \ \ \text{TMS}_2, \dots, \ \ \text{TMS}_j, \dots, \ \ \text{TMS}_{50} \right\}.$$

3. Evaluation of the Objective Function: the objective function represents the primary goal that needs to be optimized. In the context of relay coordination, it involves minimizing the total operating time of the relays while ensuring proper coordination among them. Formally, it is expressed as described by Eq. (1):

$$T = \text{Min} \sum_{j=1}^{J} W \, t_{j,k}$$

4. Position Update: The ideal outcomes from the preceding phase are used to update the locations of the solutions. The positions of the solutions are updated based on the flow of streams and rivers toward the sea (optimal solution). The position update can be mathematically modelled as:

$$TMS_j^{(t+1)} = TMS_j^{(t)} + r\left(TMS_{best}^{(t)} - TMS_j^{(t)}\right)$$

where $TMS_j^{(t)}$ is the position of the j-th solution at iteration t, $TMS_{best}^{(t)}$ is the best solution at iteration t, and r is a random number in the range [0, 1].

5. Swapping Solution Sites: To reduce local optima, solution sites are switched.
6. Introduction of Random Solutions: The likelihood of locating the ideal solution is increased by WCA's ability to prevent saturation effects and local optima.
7. Iterative Refinement: Until the maximum number of iterations is achieved, steps two through six are repeated. The iteration count determines the number of iterations the algorithm will perform, affecting the convergence and quality of the final solution. More iterations allow the algorithm to explore the search space more thoroughly but at the cost of increased computational time.

By following these steps, you may be sure that WCA will iteratively improve the solutions until it finds the best one for the OCR coordination problem. The parameters used in this study are as follows:

- Number of populations: 50
- The constant of evaporation condition: $1*10^{-5}$
- Number of streams and sea: 4
- The maximum number of iterations: 1000

4.1.2. Particle swarm optimization (PSO)

One popular and effective heuristic optimization technique that applies to a wide range of applications is the Particle Swarm Optimization (PSO) algorithm. Interestingly, it uses less memory and processing power to get the best answer [47,48]. PSO, which has its roots in the research of Kennedy and Eberhart, is influenced by both the swarming dynamics seen in animal behaviour and general human social behaviour. PSO is based on the idea of agents, or what's known as a swarm, who individually provide possible answers. Each agent keeps track of both its present location and the best place it has ever been concerning the given goal function. Agents search for better places iteratively, and from the pool of possible solutions produced in each iteration, the ideal global solution is finally assigned [47].

The PSO algorithm's benefits are used in this work to solve the coordination issue with OCRs. Initially, the ETAP simulation tool is used to model the network topology, especially an IEEE 9 BUS system in this work. Based on the IEC 60909 standard, load flow calculations and fault analysis are performed to determine the initial OCR settings. In the PSO method, these parameters represent the starting population of solutions (particles). The first step in the PSO process is to assess the population of particles that make up the solution and update their locations and trajectories according to the optimal solution found. The PSO iteration continues until the optimal solution is found and the maximum number of iterations is achieved. The parameters used in this study are as follows:

- Population size: 100
- Mutation rate: $W_{max}=0.9$ and $Wmin=0.49$
- Acceleration factors: $C1=C2=2$
- Maximum number of iterations: 100

The primary process of PSO includes iterative steps:

1- Initial Population and Velocity: A population of particles (solutions) is initialized, each with a random position and velocity: $TMS_j(0)$ and $v_j(0)$ for j =1,2,…,100
2- Evaluation of the Objective Function: Similar to WCA, the objective function in PSO for relay coordination is described in Eq. (1).
3- Update Velocity and Position: The velocity and position of each particle are updated using the best position found.
4- Adjusting Inertia Weight: The inertia weight is adjusted dynamically to balance exploration and exploitation:
5- Iterative Refinement: Steps 2 through 4 are repeated until the maximum number of iterations (100) is achieved or the optimal solution is found.

By following these steps, the PSO algorithm iteratively improves the solutions until it finds the best one for the OCR coordination problem.

4.2. Hardware-in-the-loop (HIL)

HIL testing is a methodology used in various industries, including power systems and control engineering, to validate the performance and functionality of hardware components in a simulated environment. In the context of power systems, HIL testing involves integrating physical hardware components, such as relays, protection devices, and controllers, with simulation software to emulate real-world operating conditions and verify system behaviour. This research introduces an innovative approach to tackle challenges caused by excessive fault currents, particularly in microgrid environments resulting from DG interconnection. To enhance compliance with heightened fault currents, a non-standard characteristic is proposed, considering the maximum CMS of industrial relays. These characteristics, easily programmable in numerical relays from various manufacturers, offer adaptability and versatility. By employing the WCA and PSO, this study optimizes these non-standard characteristics to achieve the security, selectivity, and reliability of OCR schemes in microgrids, particularly in islanded mode and low-fault current scenarios. To validate the effectiveness of the proposed optimization techniques and non-standard characteristics, the research integrates Hardware-in-the-Loop (HIL) testing methodology., as shown in Fig. 4. The detailed steps and components involved in HIL testing include the following steps:

1- Simulation Software: HIL testing typically begins with the selection or development of simulation software capable of accurately modelling the behaviour of the power system components under test. These tools allow for the creation of detailed models representing various elements of the power system, as follows:
   - Network Structure Implementation: The standard DN (IEEE 9 and 33 bus) with and without PV systems is modelled using ETAP and ATP/EMTP simulations.
   - Load Flow Calculation: Load flow analysis, employing the Newton-Raphson method, is performed to establish the initial current setting for each OCR, initializing relay settings.
   - Short Circuit Calculation: Short circuit calculations based on IEC 60909 standards are conducted in various scenarios to assess fault conditions.
   - Optimization Techniques Application: The configuration for the OCR system is determined using the WCA and PSO, depending on the present levels of different faults. These robust optimization methods address OCR coordination challenges effectively.
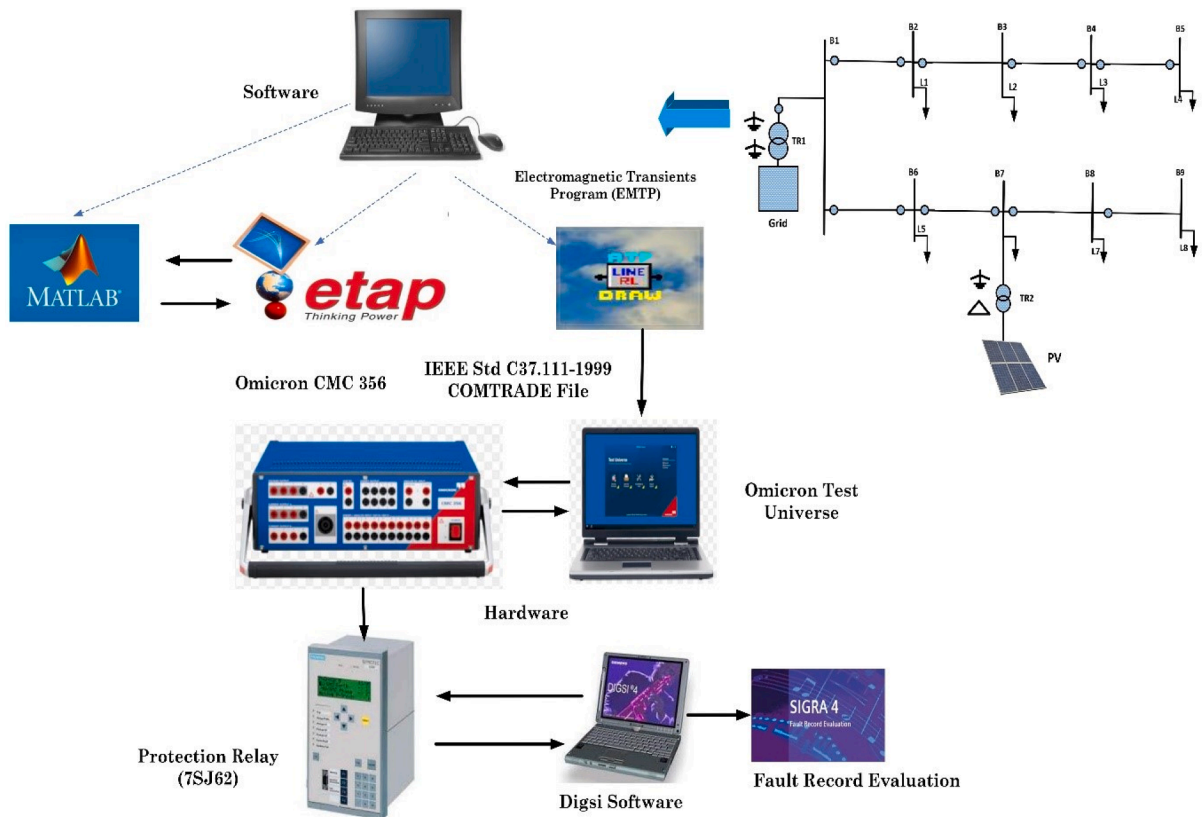

Fig. 4. Hardware-in-the-loop (HIL) testing.

- Software Implementation: The WCA and PSO algorithms are initially implemented as computer software in the MATLAB environment. Additionally, using ETAP industrial software, the effectiveness of the acquired configuration on the network protection system is validated. The ATP simulation will send the setting of testing and OCR data to the OMICRON-CMC-365, as a COMTRADE file.

2- Hardware Components: Physical hardware components, SIPROTEC 7SJ62 Multi-function Protection Relay and power testing equipment OMICRON-CMC-365 are used for integration into the HIL testing setup. These hardware components represent real-world power systems and are capable of interfacing with the simulation software. The OMICRON-CMC-365 will inject the current to the OCR (SIPROTEC 7SJ62) based on the COMTRADE file received from ATP.

3- Real-Time Simulation Platform and Interface Hardware: A real-time simulation platform is employed to execute the simulation models in real-time and synchronize them with the hardware components. The OMICRON Test Universe software is used to control, validate and reorder OMICRON-CMC-365 data. Digsi Software and Fault record evaluation are used to program the OCR (SIPROTEC 7SJ62) and validate and reorder the data.

Overall, the HIL testing will provide a powerful means of validating the performance and functionality of OCRs with different protection schemes in power systems, enabling engineers to identify and address potential issues before deployment in real-world applications.

In the following section, the performance of the proposed OCR coordination scheme within microgrids under different operation mode is investigated. The evaluation focuses on three critical parameters essential for effective protection schemes: security, selectivity, and reliability.

- Security: Ensuring that the OCRs do not operate under non-fault conditions or minor disturbances, thereby preventing unnecessary outages and maintaining system stability (miss-coordination events).
- Selectivity: The capacity of the protection scheme to isolate only the faulted section of the network while keeping the rest of the system operational. This minimizes the impact of faults and enhances the continuity of supply.
- Reliability: The overall dependability of the protection scheme to operate correctly during fault conditions. This includes both the accuracy of fault detection and the speed of response to clear the fault quickly.

By examining these parameters through detailed simulation and real-time Hardware-in-the-Loop (HIL) testing, we demonstrate how the proposed methods enhance the overall protection scheme. The results highlight the effectiveness of the optimized settings in various fault scenarios, showcasing improvements in OCR performance compared to conventional IEC standards. The proposed method employs the Water Cycle Algorithm (WCA) and Particle Swarm Optimization (PSO) techniques to optimize the Time Multiplier Setting (TMS) of OCRs, ensuring enhanced coordination and performance. The integration of Hardware-in-the-Loop (HIL) testing further validates the effectiveness of the method.

5. Simulation results and discussion

This section assesses the performance of the proposed non-standard OCRs protection scheme. The scheme is evaluated using a 9-bus DN based on the IEEE standard to gauge its effectiveness under different operational scenarios. Specifically, the performance of the scheme with different possibilities of non-standard curves and standard tripping curves (IEC) is evaluated. The testing results of the proposed scheme under fault conditions are presented, and a comparison is created with commonly used approaches in terms of total tripping time and CTI. The coordination problem is addressed using the WCA and PSO, and the results are analyzed and compared. Additionally, the proposed OCR scheme is evaluated using HIL testing to validate the performance and functionality of the OCR schemes.

5.1. Validation the of the proposed OCRs schemes

To validate the performance of the OCRs with both standard operating characteristics (Eq. (1)) and the proposed non-standard tripping characteristics (Eq. (8)), a series of short tests are conducted. These tests aimed to compare the response times and reliability of the two characteristics under various fault conditions. The standard operating characteristic follows the conventional IEC time-current characteristic curve, given in Fig. 5(a), and the proposed non-standard tripping characteristics (Eq. (8)), shown in Fig. 5 (b).

In order to validate the effectiveness and performance of the proposed non-standard tripping characteristic in comparison to the standard IEC normal inverse characteristic, a series of short tests were conducted. These tests aimed to evaluate the tripping times and overall reliability of OCRs under various fault conditions. The following sections detail the setup, fault injection process, data collection methodology, and the results obtained from these tests.

- Setup: The tests were conducted using the SIPROTEC 7SJ62 multifunction protection relays.
- Fault Injection: Various fault scenarios, including three-phase faults, were simulated to evaluate the OCR response.
- Data Collection: Tripping times were recorded for both standard and nonstandard characteristics.

The results of the short tests are summarized in Figs. 6 and 7, illustrating the validation of the non-standard characteristic and the
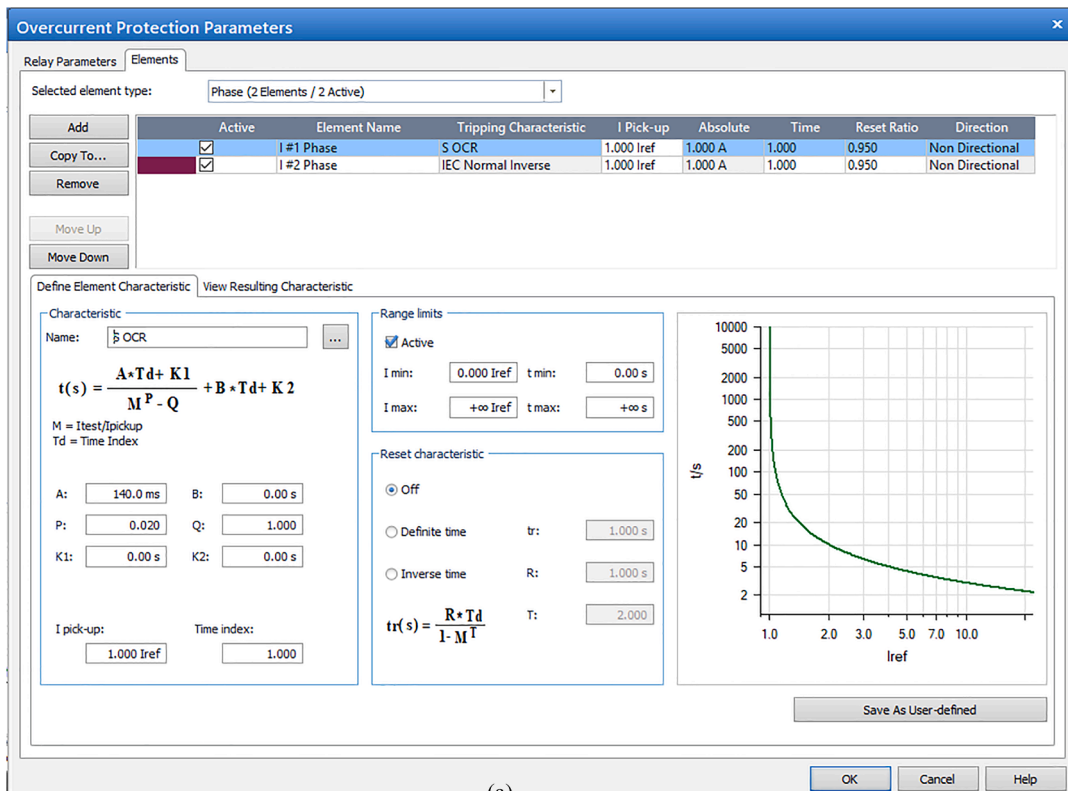
(a)
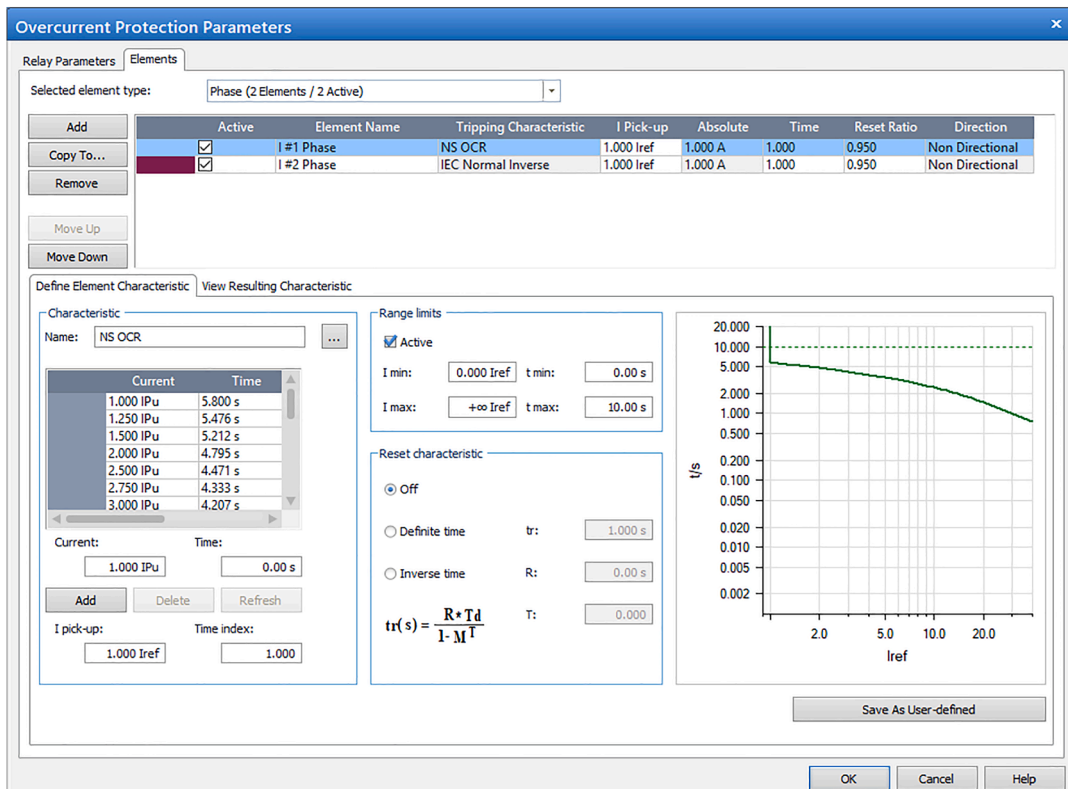
(b)

(caption on next page)

Fig. 5. The test of OCR Protection Parameters for a) standard operating characteristics (Eq. (1). b) proposed non-standard tripping characteristics (Eq. (8).

Pick-up / Drop-off Test Results:

Type	Angle	I Pick-up		I Drop-off	Reset Ratio		
		nom	act	act	nom	act	Error
L1-L2-L3	n/a	1.000 A	n/a	n/a	950.0 m	n/a	n/a

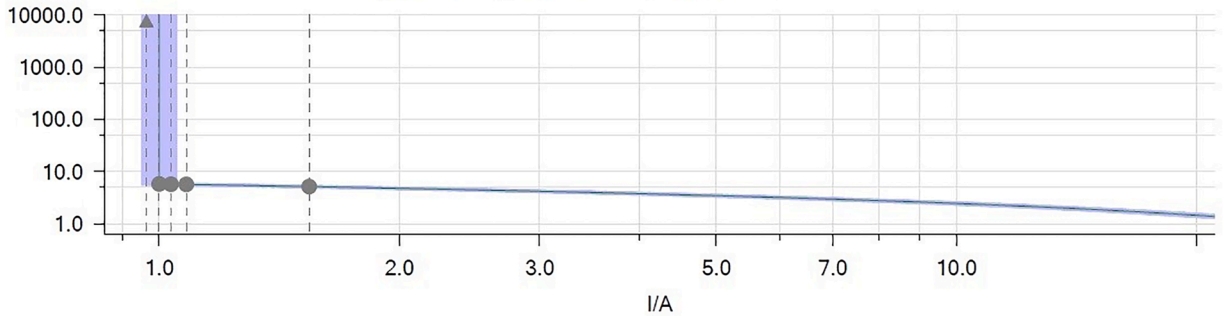| Type	Magnitude	tnom
L1-L2-L3	1.000 A	5.800 s
L1-L2-L3	964.0 m A	No trip
L1-L2-L3	1.034 A	5.750 s
L1-L2-L3	1.081 A	5.685 s
L1-L2-L3	1.542 A	5.171 s

Fig. 6. The pick-up and drop-off test results for the proposed non-standard characteristic.

Pick-up / Drop-off Test Results:

Type	Angle	I Pick-up		I Drop-off	Reset Ratio		
		nom	act	act	nom	act	Error
L1-L2	n/a	1.000 A	n/a	n/a	950.0 m	n/a	n/a

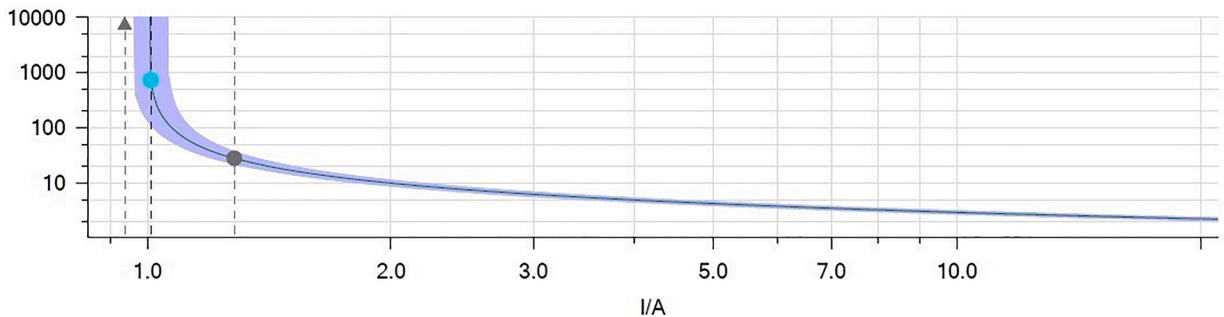| Type	Magnitude	tnom
L1-L2-L3	1.010 A	731.3 s
L1-L2-L3	937.4 m A	No trip
L1-L2-L3	1.280 A	28.26 s

Fig. 7. The pick-up and drop-off test results for the standard characteristic scheme.

standard IEC characteristic, respectively.

The short test results indicate that the proposed non-standard tripping characteristic outperforms the standard IEC characteristic in all tested fault scenarios. These findings validate the effectiveness of the proposed method and its potential for real-world applications. Figs. 6 and 7 illustrate the superior performance of the nonstandard tripping characteristic over the standard IEC characteristic,

demonstrating the effectiveness of the proposed approach in enhancing microgrid protection.

5.2. Case study

5.2.1. Description of the case study

The proposed OCRs protection schemes are tested and evaluated on a common 9-bus IEEE feeder network with and without PV systems, as shown in Fig. 8. This network is typically operated with a high-voltage/medium-voltage utility source and 4 MVA Distributed Generators (DGs) (PV farm) through a setup transformer rated at 0.4/12.4 kV. The network includes 9 OCRs protecting it from fault locations F1 to F8, representing near- and far-end fault locations from the sources. The basic settings of the OCRs, including the Current Transformer Ratio (CTR), pickup current (IP), and plug setting (PS) are established based on load flow and fault calculations according to IEC-60909, as presented in Table 2. Additionally, the performance of the proposed scheme is investigated under different DN operation models to enhance selectivity and maintain power continuity on healthy lines, as follows:

- Scenario 1: Traditional DN without PVs.
- Scenario 2: Traditional DN with PVs.

5.2.2. Case study simulation results

In this section, the performance of the suggested OCR approaches (standard and non-standard) across two different scenarios of power grid operation (with and without PV modes) are tested and compared. To assess performance, the total tripping times for OCR approaches under various fault conditions' locations are computed based on the optimal TMS, as described in Table 3. These optimal TMS values for the OCRs are determined based on the maximum load currents in each line and different fault scenarios using WCA and PSO algorithms. The TMS value aims to ensure that the primary OCRs operate as swiftly as possible to minimize tripping time and enhance grid stability. Additionally, a CTI) of 0.3 sec. is assumed between local and remote back protection to facilitate rapid coordination between OCRs.

As illustrated in Table 4, the proposed non-standard OCR approach outperformed the standard OCR scheme across all grid operation modes. For instance, under F1 conditions, the tripping time of OCR1 was reduced from 0.0226 and 0.0226 sec in Scenario 1 and 2 for the standard OCR (IEC) to 0.000981 and 0.000553 sec for non-standard approach, respectively. The non-standard curve exhibited highly sensitive performance compared to the standard curve (IEC), as demonstrated in Table 4. Thus, the most effective current-time curves for the OCR were those utilizing the non-standard curve for both grid operation scenarios.

5.2.3. Evaluation using industrial software (ETAP and ATP)

ETAP and ATP serve as common programs for protection relay testing and are also popular industrial software for applying OCR schemes in electric networks. They allow convenient assessment based on various indicators such as effectiveness, capability and feasibility of protection and energy policies. In the present work, it is used as a tool for investigating the selected OCR schemes for
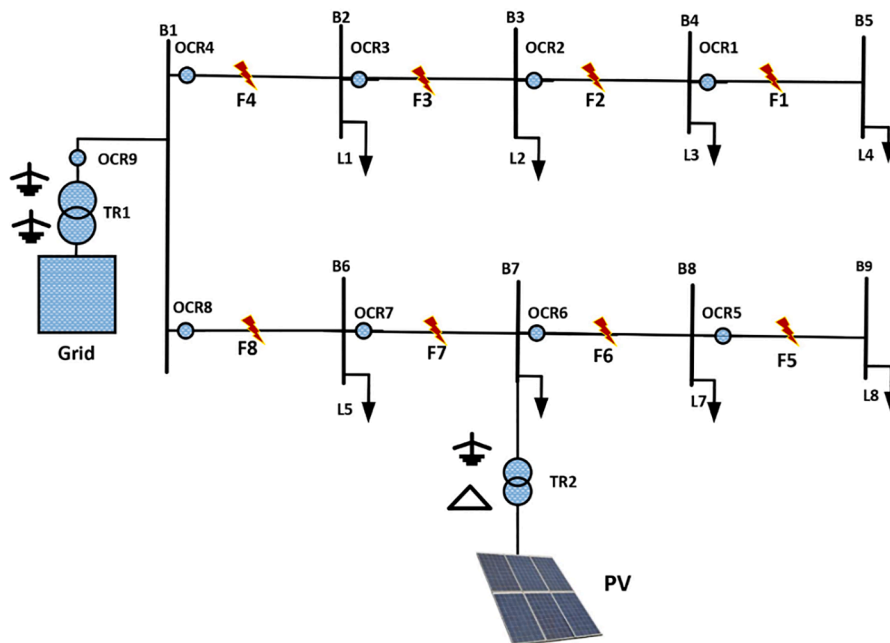

Fig. 8. Single line diagram of the IEEE 9 bus system under study.

Table 2
The OCR settings.

Relay	CTR	PS %	IP(A)
OCR1	100/1	100	100
OCR2	200/1	100	200
OCR3	300/1	100	300
OCR4	400/1	90	360
OCR5	100/1	100	100
OCR6	200/1	100	200
OCR7	300/1	100	300
OCR8	400/1	100	400
OCR9	800/1	100	800

Table 3
The TMS settings for the OCRs schemes (standard and non-standard) under different grid operation modes.

Relay	Scenario 1 (Without PV)				Scenario 2 (With PV)			
	Standard		Non-standard		Standard		Non-standard	
	PSO	WCA	PSO	WAC	PSO	WCA	0.01	WAC
OCR1	0.01	0.01	0.01	0.01	0.01	0.01	0.3	0.010
OCR2	0.142	0.142	0.29	0.102	0.142	0.142	0.4	0.103
OCR3	0.258	0.255	0.389	0.184	0.258	0.259	0.49	0.185
OCR4	0.349	0.344	0.478	0.262	0.349	0.350	0.01	0.263
OCR5	0.01	0.01	0.01	0.010	0.01	0.010	0.31	0.011
OCR6	0.142	0.142	0.339	0.104	0.142	0.142	0.38	0.105
OCR7	0.254	0.266	0.471	0.190	0.254	0.254	1.27	0.185
OCR8	3.00	1.597	3	0.353	3.00	1.457	0.42	0.339
OCR9	0.352	0.360	0.417	0.313	0.352	0.353	0.01	0.314

Table 4
The tripping time of the OCRs (standard and non-standard) under different grid operation modes across different fault locations.

Fault Current	OCR	Fault Current - Scenario 1	Tripping Time (s) - Scenario 1		Fault Current - Scenario 2	Tripping Time (s) - Scenario 2	
			Standard	Non-standard		Standard	Non-standard
F1	OCR 1	4378	0.0226	0.000981	4519	0.0226	0.000553
	OCR 2	4378	0.32092	0.299819	4519	0.32092	0.29732
F2	OCR 2	4882	0.33112	0.25716	5063	0.31092	0.251284
	OCR 3	4882	0.62852	0.575179	5063	0.6192	0.553997
F3	OCR 3	5496	0.60114	0.495667	5707	0.5934	0.48834
	OCR 4	5496	0.9074	0.794713	5707	0.89434	0.792743
F4	OCR 4	6246	0.86203	0.712166	6445	0.85156	0.709298
	OCR 9	6246	1.17216	1.01149	6186	1.1972	0.94889
F5	OCR 5	4378	0.0226	0.000981	4599	0.0226	0.000316
	OCR 6	4882	0.32092	0.300612	4599	0.32092	0.299887
F6	OCR 6	4882	0.32092	0.300612	5057	0.32092	0.260157
	OCR 7	5496	0.59182	0.600152	4841	0.61976	0.549299
F7	OCR 7	5496	0.59182	0.600152	5496	0.59182	0.484199
	OCR 8	6246	7.41	4.46966	5496	3.77	2.111476

minimum tripping time and preventing wrong trips during a group operation. A simulator modal is developed to display an OCR arrangement with optimal coordination using ETAP for Scenario 1 and Scenario 2 under different locations with an application of the WCA algorithm. According to Figs. 9 and 10, the time domain simulation should show the coordination between primary and secondary OCRs in the time domain. Fig. 9 shows the coordination between primary and secondary OCRs for the standard and non-standard schemes during F2 (4.882 kA) under Scenario 1. The proposed non-standard OCR approach outperformed the standard OCR scheme, where the tripping time of OCR2 and OCR3 were reduced from 0.331 and 0.628 sec in primary and secondary OCRs for the standard OCR (IEC) to 0.257 and 0.575 sec for non-standard approach, respectively. Similarly, the proposed non-standard OCR approach recorded the minimum tripping time compared to the standard OCR scheme under Scenario 2, as shown in Fig. 10. The tripping time of OCR3 and OCR4 were reduced from 0.593 and 0.894 sec in primary and secondary OCRs for the standard OCR (IEC) to 0.488 and 0.79 sec for non-standard approach, respectively.

Transient phenomena are temporary events that can occur in real power systems due to various factors such as switching processes or faults. To examine how power networks and the proposed OCR schemes respond to such events, this study employs the ATP Simulation, as depicted in Fig. 8. ATP is widely used in the fields of power systems and power electronics to analyze transient
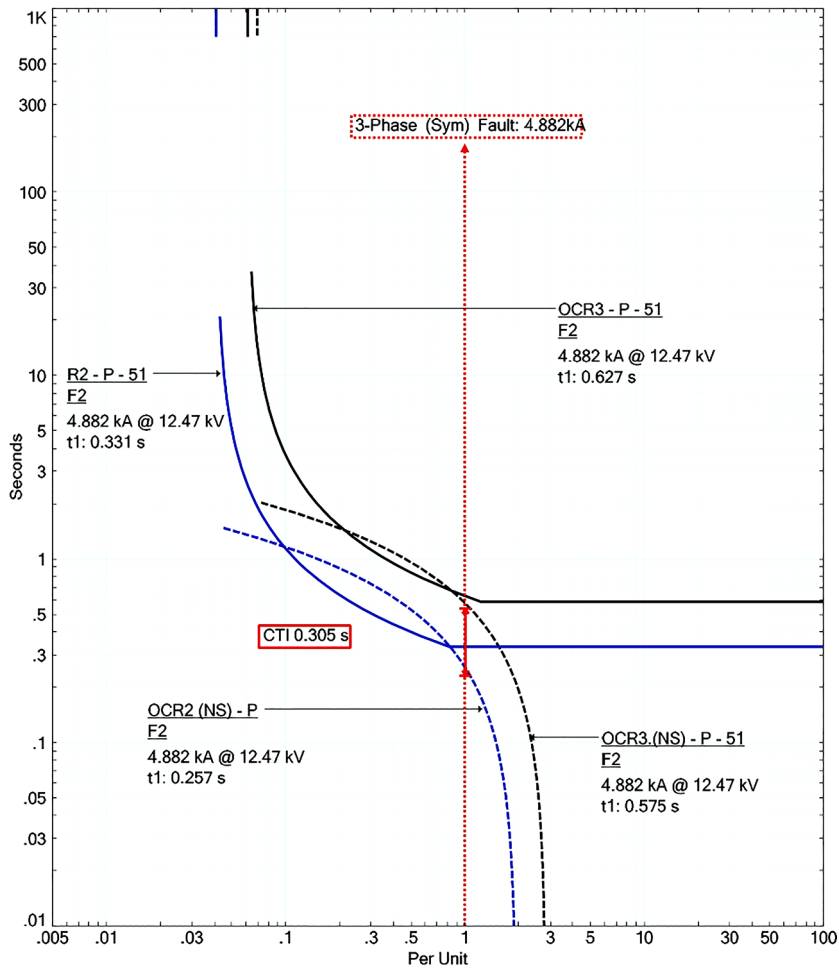
Fig. 9. Time characteristics curves of OCRs schemes for Scenario 1 under F2.

behaviour [28]. This simulation tool involves modelling network equations using differential equations and accounting for different electrical conditions. Capacitive and inductive elements in ATP exhibit frequency-dependent reactance characteristics, requiring detailed models for electrical components and controllers [28,29]. With time intervals as short as 50 microseconds, ATP accurately captures the rapid dynamics within power systems induced by devices like voltage source converters. In power networks with PVs, converters play a crucial role in linking PVs to distribution grids. ATP simulations are essential for studying the integration of renewables into modern power networks, including tasks such as protective mechanism coordination. Moreover, within the domain of electromagnetic transient phenomena, the operation time scales of power protection relays are critical considerations. Fig. 8 shows the proposed standard and non-standard OCR approaches under Scenario 1 for OCR 9 at F4. The non-standard recorded the minimum tripping time compared to the standard OCR scheme, as shown in Fig. 11. The tripping time of OCR9 was 0.948 seconds as secondary OCR, while the standard OCR (IEC) was 1.19 sec.

5.2.4. Convergence characteristic of WCA and PSO

Convergence curves give us an intrinsic understanding of the algorithm's behaviour in the optimization process, which shows how the algorithm performs gradually over iterations. In Fig. 12, where the converge graph for Scenario 1 is continued to exhibit for both algorithms WCA is shown to rank the best because it is characterized by a smooth and fast convergence. When considering the process similarity between the WCA convergence curve and PSO (See Fig. 13), what becomes evident is that WCA reaches the optimal solution in a highly efficient way. Indeed, it derives its concave curve to get to the goal function optimum very quickly and stresses very high performance of both times of convergence and convergence speed. This means that WCA is more powerful at solving the proposed OCR coordination problem compared to PSO. This can be achieved by WCA having the ability to conduct a smaller number of iterations before reaching the optimal solution, thereby resulting in the offloading or reducing the computational necessity of the CPU. This is especially important for tasks that require the optimized function with limited computational resources or in cases where the optimizer`s working time is critical. The main advantage of the WCA algorithm is its fast convergence, which not only expedites the optimization process but also cuts down on the total computer consumption, therefore, the algorithm is more likely a perfect candidate
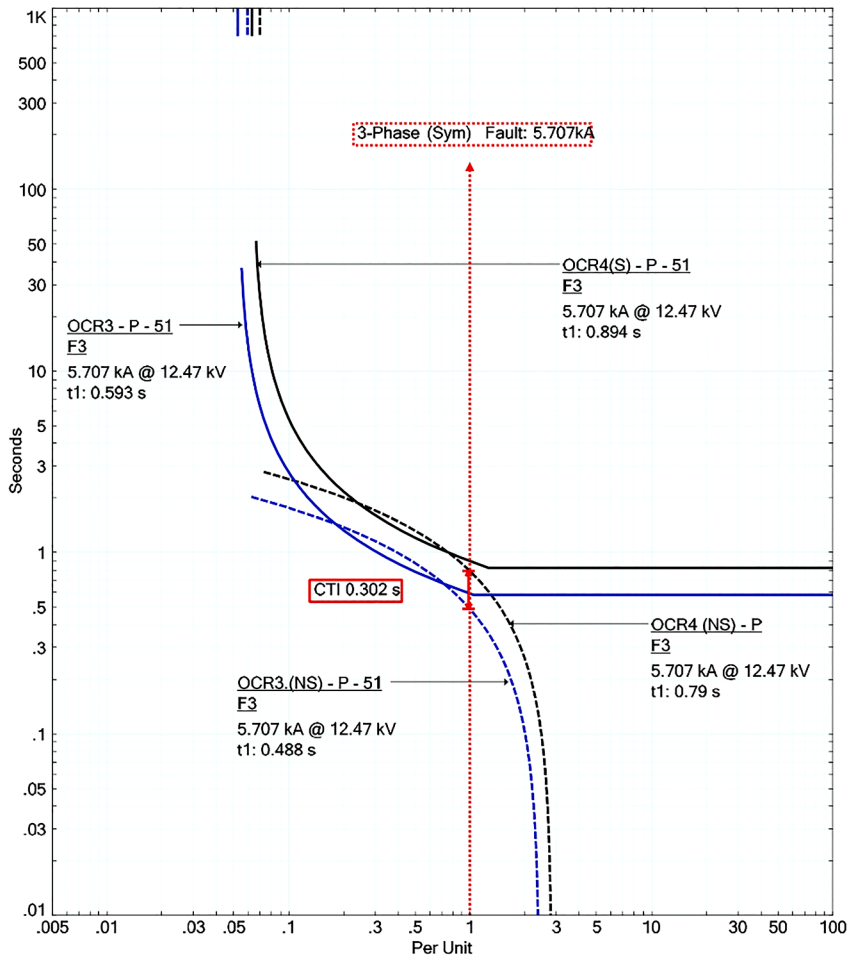
Fig. 10. Time characteristics curves of OCRs schemes for Scenario 2 under F3.

for dealing with OCR coordination computing problems shortly compared to PSO.

5.3. The impact of PV and wind systems location and size on the protection schemes

The performance of the proposed OCRs protection schemes is evaluated on a common 9-bus IEEE feeder network with different size and location of PV and wind systems (WT), as shown in Fig. 14. This network is typically operated with different DGs (PV and wind systems) through a setup transformer rated at 0.4/12.4 kV. The placement and size of PV compared to section 5.1 and wind systems significantly influence the performance and reliability of protection schemes in the network. The addition of PV and WT systems can introduce variability in power flow and fault current levels, affecting the settings and coordination of OCRs. Each scenario (A, B, and C) presents a different operational configuration, leading to variations in the network's response to faults.

- Scenario A (PV): The system relies heavily on PV sources (two of 4 MW PV farms), impacting fault current levels at TR2 and TR3, potentially requiring recalibration of OCR settings around these buses.
- Scenario B (WT1): With WT1 online and both PV systems offline, the fault current contribution from WT1 at TR2 becomes critical, affecting the OCRs at B7 and adjacent buses.
- Scenario C (WTs dominant): Both wind turbines are operational, introducing fault currents from at TR2 and TR3. The protection scheme needs to accommodate these contributions while ensuring reliable operation of OCRs.

The network includes 9 OCRs protecting it from fault locations F1 to F8, representing near- and far-end fault locations from the sources. The basic settings of the OCRs (TMS) is established based on load flow and fault calculations according to IEC-60909, as presented in Table 5.

The analysis and comparison of OCR coordination approaches based on the fault current and OCR tripping time results, as described in Table 6, shows important insights. Fault currents increase progressively from Scenario A to Scenario C due to the varying
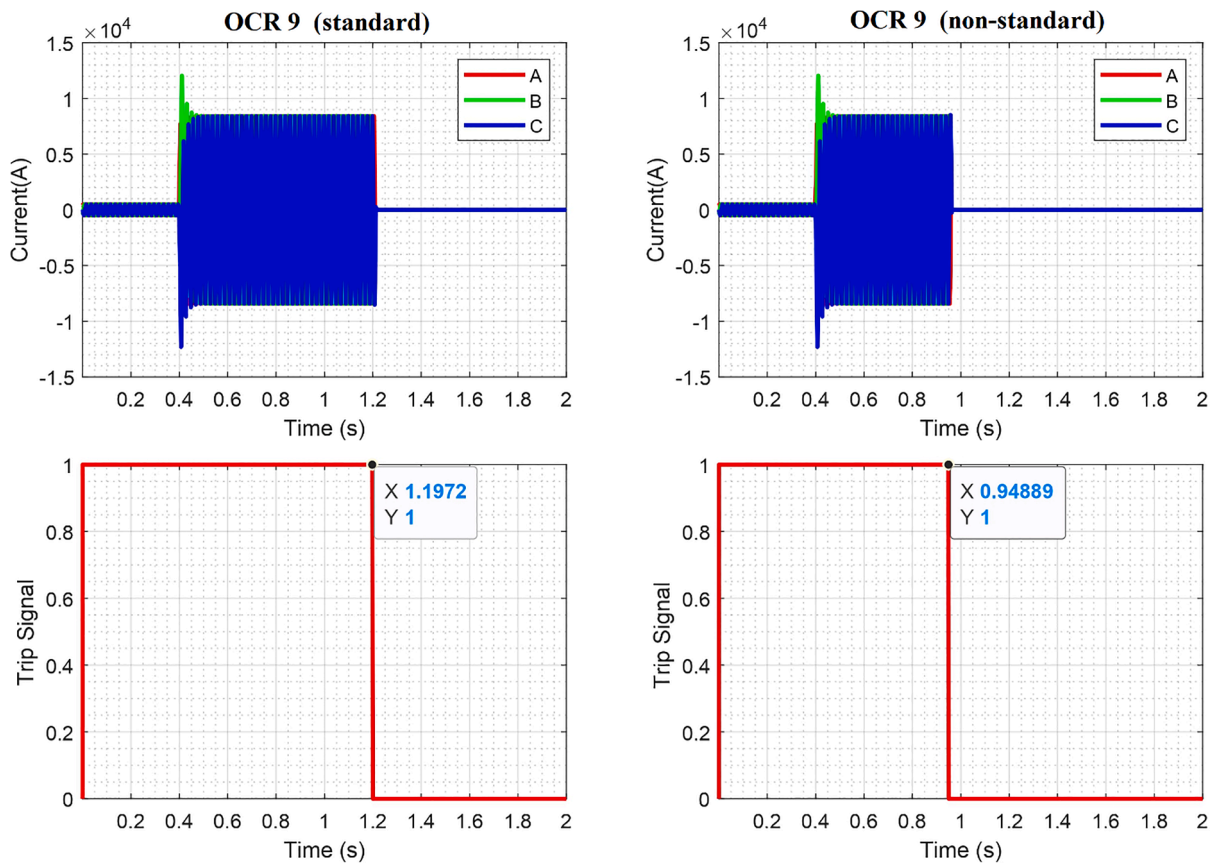
Fig. 11. The current at OCR under standard and non-standard schemes with trip signals.
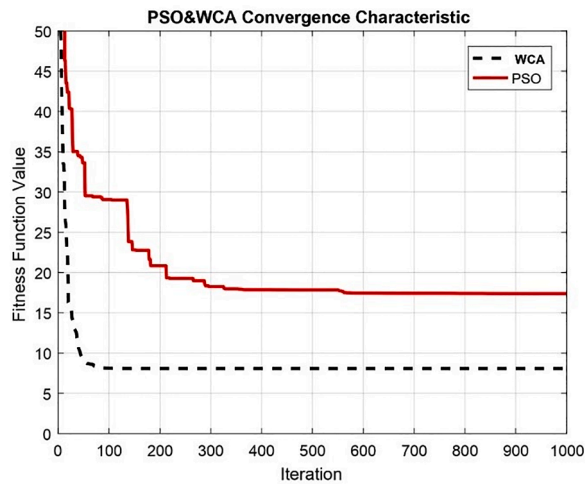

Fig. 12. Convergence characteristic of WCA and PSO at Scenario 1.

contributions of the PV and WT systems in each scenario. For instance, at F1, the fault current increases from 4635A in Scenario A to 5176A in Scenario C. The presence and configuration of PV and WT systems significantly impact fault currents and relay operations. For instance, at F4, the fault current increases substantially from 6652A in Scenario A to 8159A in Scenario C, necessitating careful consideration of relay settings to avoid miss-operation or delayed tripping. Both standard and non-standard protection schemes handle fault conditions, but non-standard settings show higher performance in tripping times in some cases, such as at F2 with OCR2, where the non-standard tripping time in Scenario A is 0.286 s compared to 0.291 s for the standard setting. Scenario-based analysis shows that
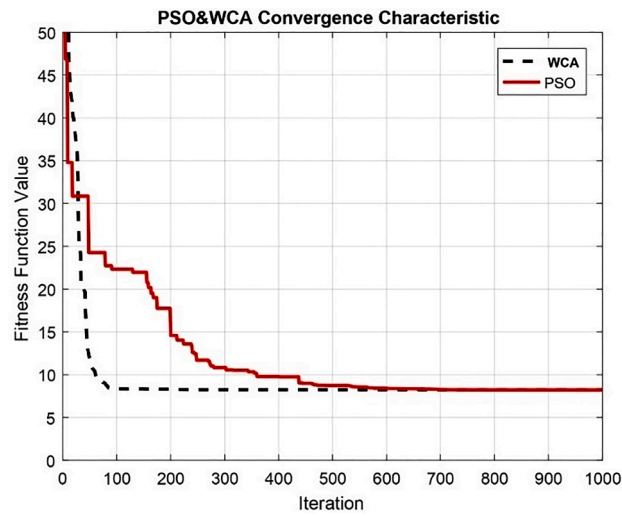
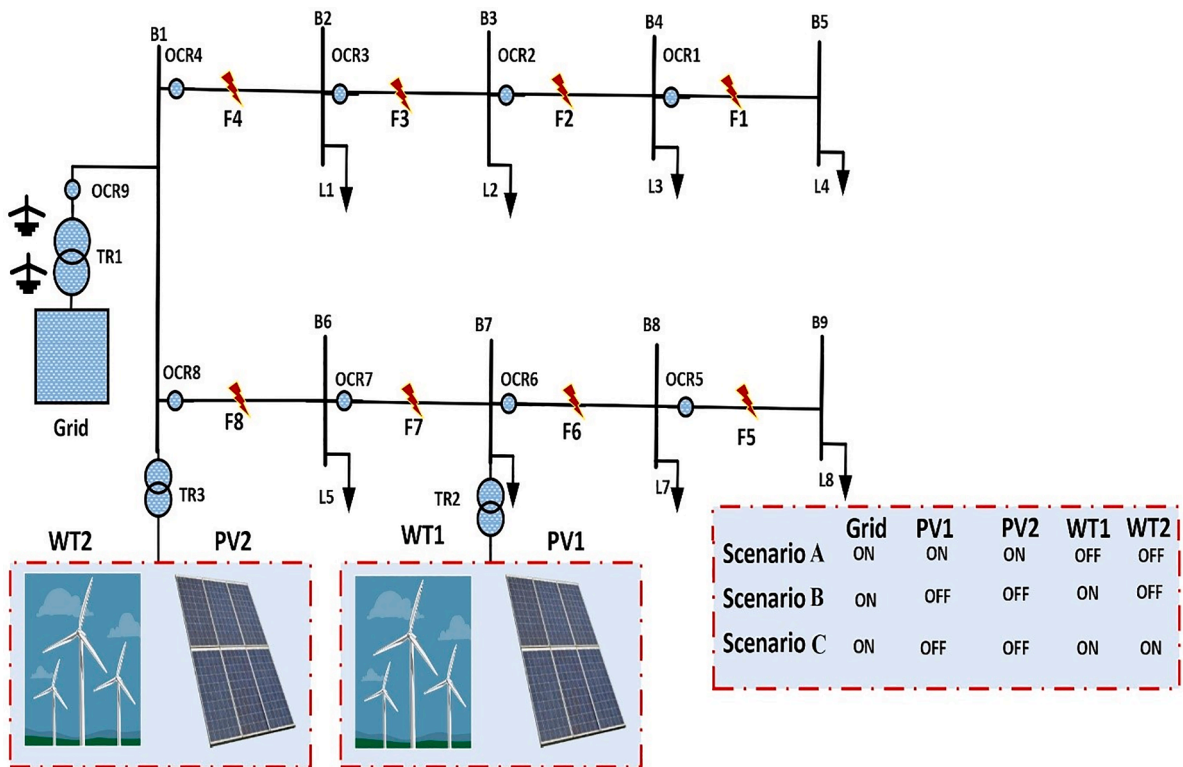**Fig. 13.** Convergence characteristic of WCA and PSO at Scenario 2.

Fig. 14. IEEE 9 bus system with different operation grid modes and DGs.

in Scenario A (PV), fault currents are lower, and tripping times are slightly shorter, indicating effective protection. However, careful monitoring is required to ensure relays are not too sensitive. In Scenario B (WT1), increased fault currents necessitate robust protection settings. OCRs handle the increased currents well, but non-standard settings show improvements in tripping times. Scenario C (WTs) experiences the highest fault currents, requiring both standard and non-standard settings to be optimized to handle these conditions without compromising protection reliability.

Table 5

The TMS settings for the OCRs schemes (standard and non-standard) under different grid operation modes.

Relay	Scenario A (8 MVA – PV systems)		Scenario B (4 MVA – Wind system)		Scenario C (8 MVA – Wind systems)	
	Standard	Non-standard	Standard	Non-standard	Standard	Non-standard
TMS						
OCR1	0.01	0.01	0.01	0.01	0.01	0.01
OCR2	0.14	0.11	0.143	0.113	0.152	0.118
OCR3	0.25	0.175	0.25	0.18	0.28	0.187
OCR4	0.36	0.255	0.36	0.26	0.394	0.267
OCR5	0.01	0.01	0.01	0.01	0.01	0.01
OCR6	0.142	0.106	0.146	0.11	0.15	0.115
OCR7	0.24	0.175	0.24	0.17	0.25	0.178
OCR8	0.334	0.254	0.334	0.248	0.346	0.257
OCR9	0.335	0.262	0.329	0.259	0.335	0.253

Table 6

The tripping time of the OCRs (standard and non-standard) under different grid operation modes across different fault locations.

Fault Current	OCR	Fault Current - Scenario A	Tripping Time (s) - Scenario A		Fault Current - Scenario B	Tripping Time (s) - Scenario B		Fault Current - Scenario C	Tripping Time (s) - Scenario C	
			Standard	Non-standard		Standard	Non-standard		Standard	Non-standard
F1	OCR 1	4635	0.01	0.01	4794	0.01	0.01	5176	0.01	0.01
	OCR 2	4635	0.302	0.303	4794	0.305	0.306	5176	0.308	0.308
F2	OCR 2	5193	0.291	0.286	5418	0.294	0.288	5922	0.30	0.286
	OCR 3	5193	0.596	0.581	5418	0.594	0.587	5922	0.60	0.587
F3	OCR 3	5854	0.572	0.552	6202	0.56	0.554	6888	0.606	0.549
	OCR 4	5854	0.879	0.859	6202	0.86	0.885	6888	0.907	0.841
F4	OCR 4	6652	0.839	0.815	7197	0.816	0.803	8159	0.856	0.78
	OCR 9	6123	1.130	1.11	6089	1.11	1.10	5935	1.15	1.08
F5	OCR 5	4744	0.01	0.01	5212	0.01	0.01	5607	0.01	0.01
	OCR 6	4744	0.30	0.307	5212	0.303	0.304	5607	0.305	0.307
F6	OCR 6	5294	0.289	0.291	5941	0.291	0.285	6475	0.292	0.284
	OCR 7	4996	0.581	0.59	4758	0.591	0.584	5318	0.591	0.585
F7	OCR 7	5676	0.555	0.560	5496	0.561	0.551	6249	0.559	0.546
	OCR 8	5676	0.850	0.868	5496	0.869	0.859	6249	0.857	0.845

5.4. Hardware-in-the-loop (HIL) testing results

Real-Time Simulation Platform and Interface Hardware: A real-time simulation platform is employed to execute the simulation models in real-time and synchronize them with the hardware components. The OMICRON Test Universe software is used to control, validate and reorder OMICRON-CMC-365 data. Digsi Software and Fault record evaluation are used to program the OCR (SIPROTEC 7SJ62) and validate and reorder the data. In this work, the HIL testing methodology is integrated to validate the proposed OCR schemes in real-time scenarios, as outlined in Fig. 4 and described in Section 4.2. This process involves real-time validation of results using OMICRON-256 on SIPROTEC 7SJ62 Multi-function Protection Relay, confirming the efficacy of the proposed WCA. Validation is conducted using computerized test sets and multifunction relay SIPROTEC 7SJ62. The HIL testing setup incorporates physical hardware components, including the SIPROTEC 7SJ62 and power testing equipment OMICRON-CMC-365. Furthermore, a real-time simulation platform is utilized to execute simulation models in real time and synchronize them with hardware components. In addition, Digsi Software and Fault record evaluation are used to program the OCR (SIPROTEC 7SJ62) and validate and record the data generated during the testing in this section. Fig. 15 presents the HIL testing results for OCR2 with the standard scheme at Scenario 2. The recorded fault current was 5065 A and the OCR2 tripped at time 0.312 sec. In Fig. 15, HIL testing results for OCR2 with a non-
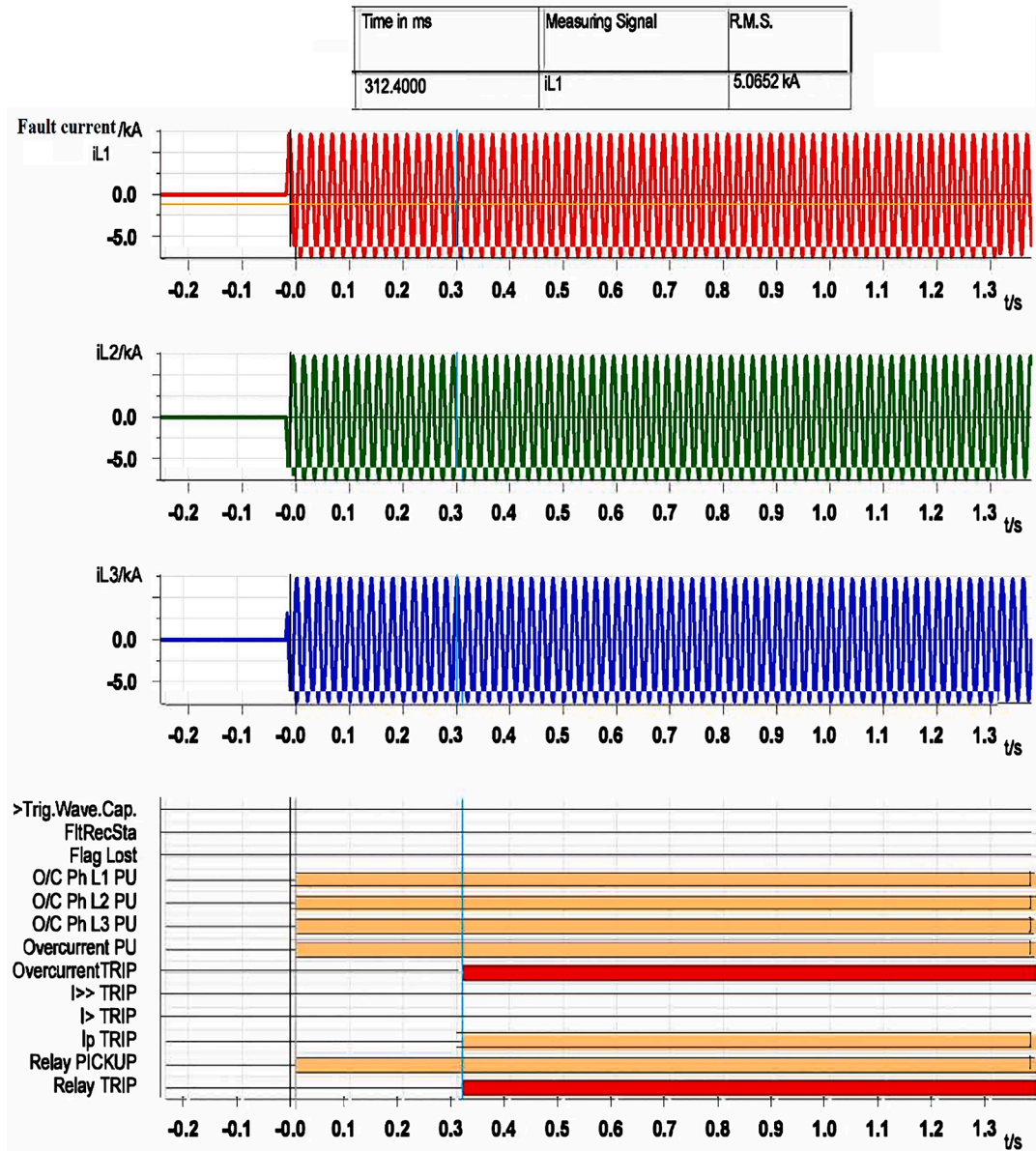
Time in ms	Measuring Signal	R.M.S.
312.4000	iL1	5.0652 kA

Fig. 15. Hardware-in-the-Loop (HIL) testing results for OCR2 with standard scheme at Scenario 2.

standard scheme at Scenario 2. The HIL results showed that the non-standard scheme outperformed the standard scheme and recorded minimum tripping time. The tripping time for OCR2 with the non-standard scheme at Scenario 2 was 0.261 sec under fault equal to 5064 A, as shown in Fig. 16. This example of HIL corroborated the findings obtained from simulations conducted in previous sections, further validating the effectiveness of the proposed non-standard compare to standard characteristics. This result demonstrates the consistency between simulated outcomes and real-world performance, reinforcing the reliability and applicability of the proposed methodologies. By integrating HIL testing into the validation process, the research ensures a comprehensive assessment of the proposed techniques and their practical viability in real-time scenarios. This alignment between simulated and real-world results highlights the robustness of the proposed approach and enhances confidence in its potential implementation within power grid protection schemes.

5.5. Limitation of current multiplier setting (CMS) results

The protection coordination performance of OCRs is crucial in ensuring the reliability and stability of power distribution systems. One of the most commonly used protection characteristics is the Inverse Characteristics (standard scheme), which is designed to trip faster as the current increases. However, this standard scheme has limitations, particularly when dealing with fault currents exceeding
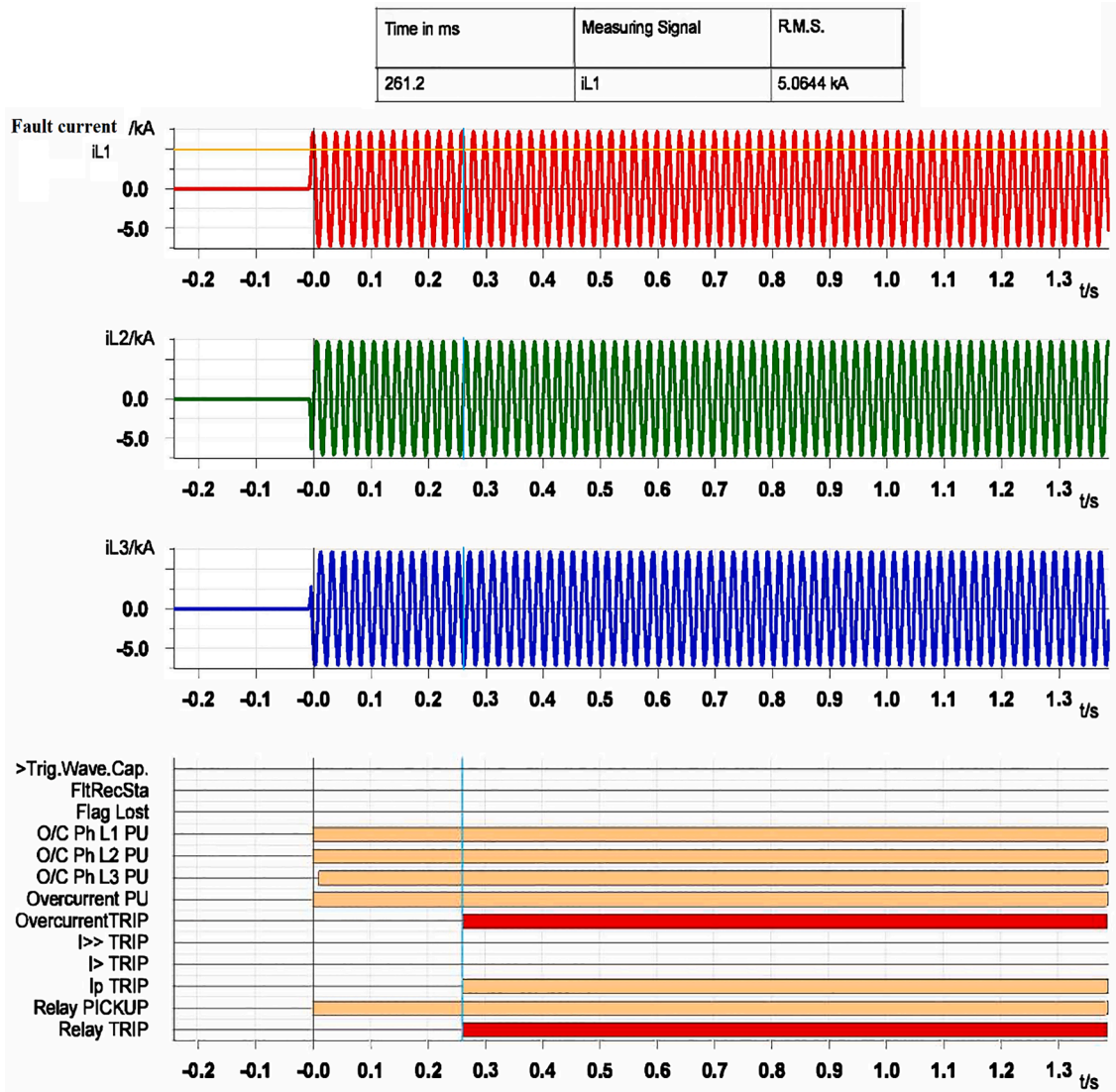
Time in ms	Measuring Signal	R.M.S.
261.2	iL1	5.0644 kA

Fig. 16. Hardware-in-the-Loop (HIL) testing results for OCR2 with non-standard scheme at Scenario 2.
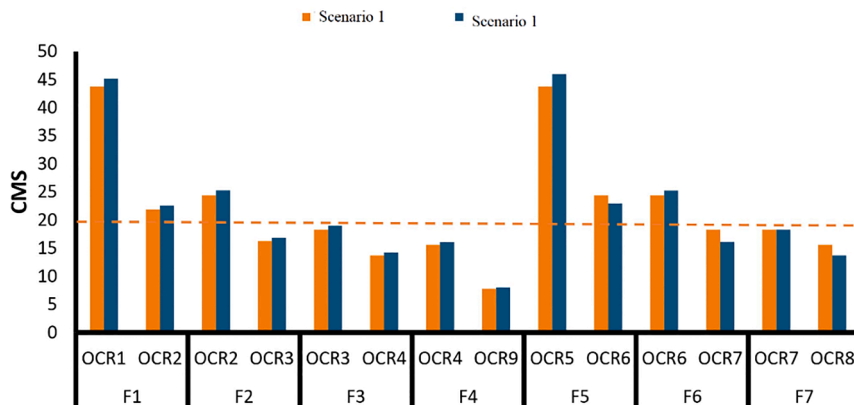

Fig. 17. Current Multiplier Setting (CMS) for OCRs under different fault locations.

a certain level, denoted as the Current Multiplier Setting (CMS). For CMS values greater than 20, the standard OCR scheme may operate within a definite time region, leading to potential mis-coordination events due to instantaneous tripping or delayed coordination. Therefore, the non-standard OCR scheme is proposed and employed in this work, as discussed in Section 3. Fig. 17 shows the CMS levels for all OCRs under different fault locations for power networks with and without PVs. With the integration of PVs into power networks, the fault current level increases in most cases compared to the grid without PVs. In addition, the CMS exceeds the 20 level in 4 cases at faults F1, F2, F5 and F6.

The proposed non-standard OCR approach outperformed the standard OCR scheme across all cases where CMS is more than 20. For instance, under F2 conditions, the tripping time of OCR2 was reduced from 0.331 and 0.310 sec in Scenario 1 and 2 for the standard OCR (IEC) to 0.257 and 0.251 sec for the non-standard approach, respectively. The non-standard curve exhibited highly sensitive performance compared to the standard curve (IEC), as demonstrated in Table 7. Thus, the most effective current-time curves for the OCR were those utilizing the non-standard curve for both grid operation scenarios. Fig. 18 shows the Time characteristics curves of OCR 6 schemes for Scenario 2 under F6. The proposed non-standard OCR approach outperformed the standard OCR scheme, where the tripping time was 0.26 sec for the non-standard, while the standard curve was 0.3292 sec and operated in the definite time region.

5.6. Large scale power system

This section employs the IEEE 33-bus distribution network model to evaluate and compare the standard to non-standard schemes. The objective is to demonstrate the adaptability and effectiveness of the non-standard scheme across different distribution networks. Fig. 19 describes the IEEE 33-bus system, ensuring that each bus voltage remains within 10 % of its nominal value. The network is fed by the utility system and incorporates on 5-MW solar power plant. To assess the initial configuration, Table 8 presents the current transformer ratio (CTR), PS, IP and TMS for each OCR within the IEEE 33-bus system. By simulating three-phase faults, this study aims to validate the performance of the proposed non-standard scheme and establish its applicability to various distribution networks.

The tripping times for primary and backup OCR pairs for both the standard and non-standard schemes during various fault scenarios are detailed in Table 9. The results show that the non-standard OCR consistently provides shorter tripping times compared to the standard characteristic across all fault scenarios. In addition, as the fault current increases, the advantages of the non-standard characteristic become more highlighted. For example, during Fault 3 (F3) with a fault current of 1382 A, OCR 3′s tripping time is reduced from 0.59 sec (standard) to 0.38 sec (non-standard), and OCR 4′s time decreases from 0.90 sec to 0.68 sec. This trend continues across subsequent faults, with significant reductions in tripping times for higher fault currents. The non-standard characteristic demonstrates a consistent ability to shorten tripping times across various fault scenarios, enhancing the overall efficiency and reliability of the protection system. Table 10 shows that the non-standard characteristic reduced the total tripping time for all OCRs from 35.869 sec to 18.816 sec. This improvement in response time is crucial for minimizing damage and reducing system downtime, thereby ensuring more reliable protection coordination.

Fig. 20 shows the coordination between primary and secondary OCRs for the standard and non-standard schemes during F17 (5970 A). The proposed non-standard OCR approach outperformed the standard OCR scheme, where the tripping time of OCR20 and OCR21 were reduced from 0.603 and 0.907 sec in primary and secondary OCRs for the standard OCR (IEC) to 0.133 and 0.435 sec for non-standard approach, respectively.

6. Conclusions and recommendations

In general, this study has proposed modern optimization techniques and non-standard characteristics for enhancing the coordination and performance of OCRs in power grid protection schemes. Through the utilization of advanced optimization algorithms such as the WCA and PSO coupled with the integration of HIL testing methodology, the effectiveness of the proposed techniques has been thoroughly investigated and validated. The results obtained from simulations and HIL testing demonstrate the superiority of the proposed non-standard approach in achieving optimal coordination of OCRs, particularly in scenarios involving PV interconnection and transient phenomena. By optimizing parameters such as TMS and coordination time intervals, the proposed techniques offer enhanced selectivity, reliability, and security in microgrid protection. Based on the findings of this study, several recommendations can be made for future research and practical implementation:

- The integration of machine learning and artificial intelligence algorithms could enhance the predictive capabilities of OCR coordination schemes, leading to more efficient fault detection and isolation.
- Collaboration with industry stakeholders and utilities is essential to validate the proposed new techniques in real-world microgrid environments and to assess their scalability and interoperability with existing protection systems.
- Continued investment in HIL testing facilities and simulation tools is crucial to support the development and validation of advanced microgrid protection schemes, ensuring their reliability and effectiveness under various operating conditions.

By addressing these recommendations, future research actions can further advance the state-of-the-art in microgrid protection and contribute to the development of robust and resilient energy systems.

Declarations

All persons who meet authorship criteria are listed as authors, and all authors certify that they have participated sufficiently in the

Table 7

The tripping time of the OCRs (standard and non-standard) under CMS is more than 20.

| Fault Current	OCR	Fault Current - Scenario 1	Tripping Time (s) Scenario 1		Fault Current - Scenario 2	Tripping Time (s) Scenario 2	
			Standard	Non-standard		Standard	Non-standard
F1	OCR 1	4378	0.022	0.0009	4519	0.022	0.0005
	OCR 2	4378	0.320	0.299	4519	0.320	0.297
F2	OCR 2	4882	0.331	0.257	5063	0.31092	0.251
F5	OCR 5	4378	0.022	0.0009	4599	0.0226	0.0003
	OCR 6	4882	0.320	0.300	4599	0.32092	0.299
F6	OCR 6	4882	0.320	0.300	5057	0.3292	0.260
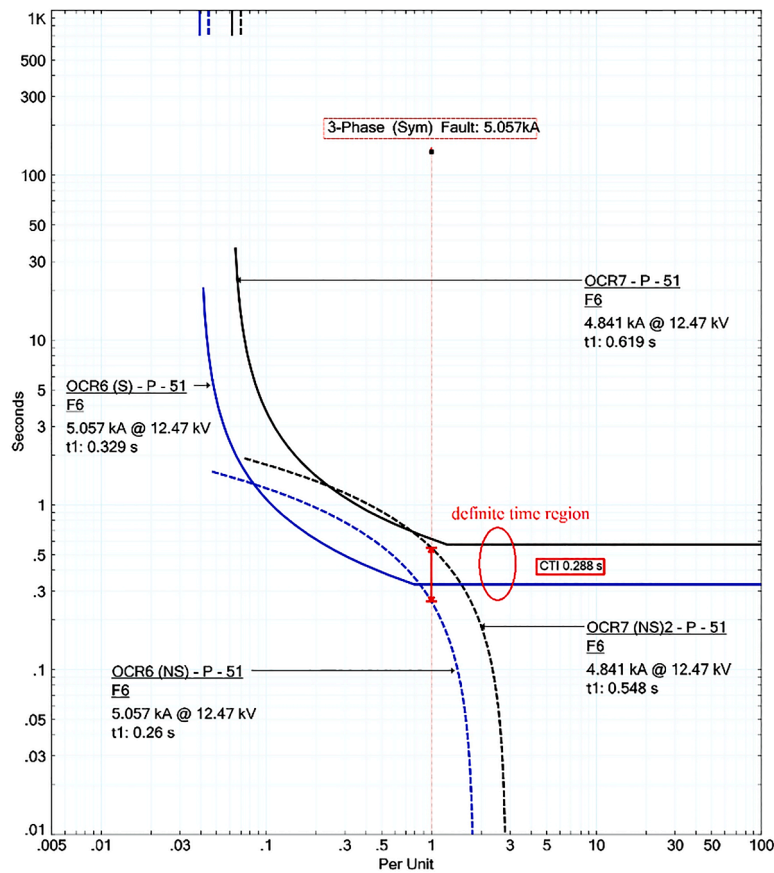
Fig. 18. Time characteristics curves of OCRs schemes for Scenario 2 under F6.

work to take public responsibility for the content, including participation in the concept, design, analysis, writing, or revision of the manuscript. We also confirm that all authors have participated in drafting the article or revising it critically for important intellectual content; and approval of the final version.

Ethical approval

Not applicable.

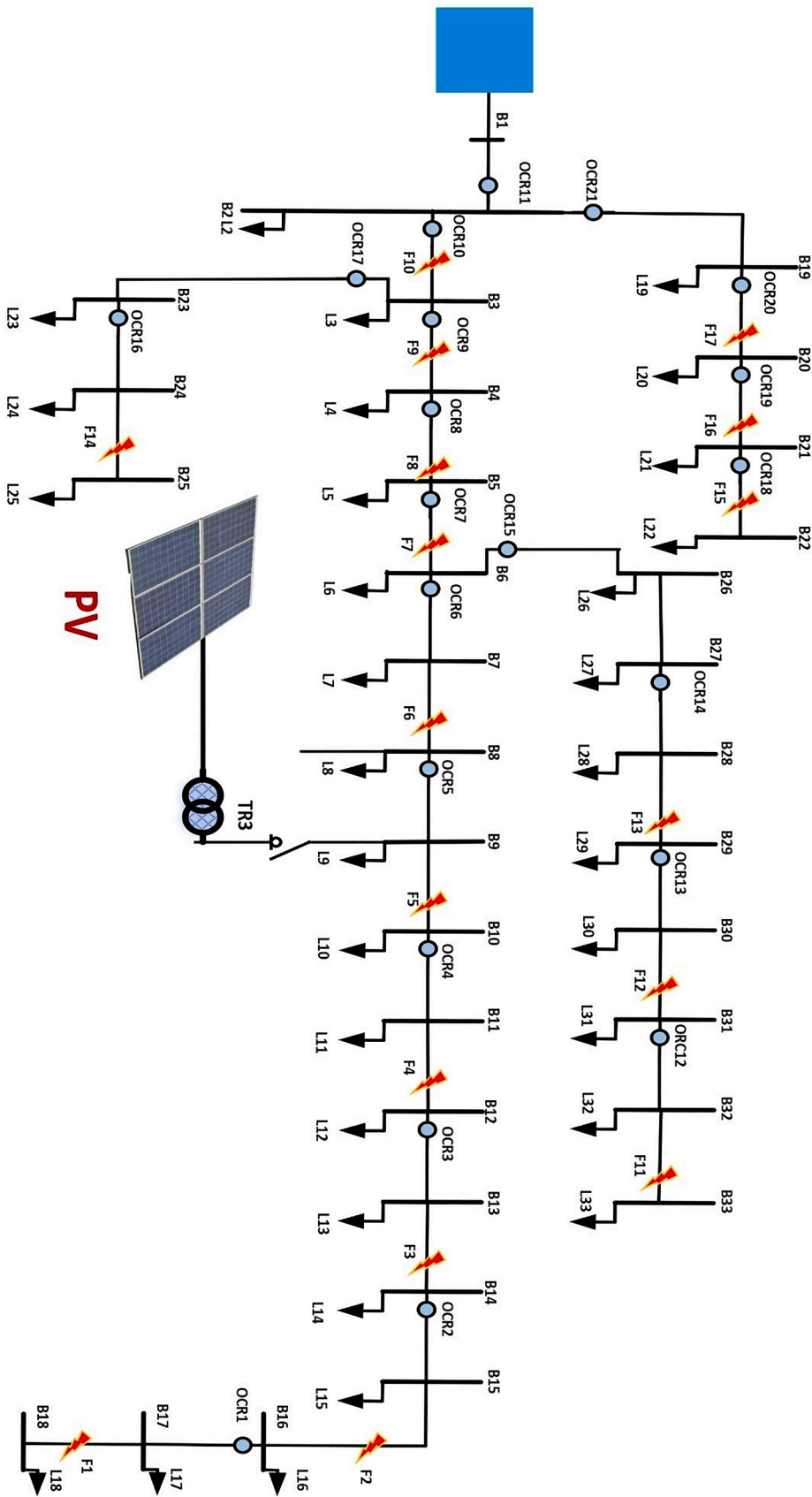**Funding**

(caption on next page)

25

Fig. 19. Large scale network, IEEE 33-BUS.

Table 8
Main model and protection scheme parameters: CTR, PS%, IP and TMS for each OCR.

Relay	CTR	PS %	IP(A)	TMS	
				Standard	Non-standard
OCR1	100/1	20	20	0.01	0.01
OCR2	100/1	20	20	0.135	0.13
OCR3	100/1	20	20	0.26	0.3
OCR4	100/1	50	50	0.4	0.27
OCR5	100/1	50	50	0.532	0.4
OCR6	100/1	80	80	0.64	0.365
OCR7	100/1	80	80	0.77	0.05
OCR8	100/1	80	80	0.91	0.07
OCR9	100/1	80	80	1.02	0.94
OCR10	200/1	100	200	1.15	0.51
OCR11	300/1	100	300	1.29	0.522
OCR12	100/1	20	20	0.06	0.06
OCR13	100/1	50	50	0.19	0.13
OCR14	100/1	50	50	0.325	0.25
OCR15	100/1	50	50	0.45	0.39
OCR16	100/1	50	50	0.01	0.01
OCR17	100/1	50	50	0.133	0.16
OCR18	100/1	20	20	0.01	0.01
OCR19	100/1	20	20	0.135	0.38
OCR20	100/1	50	50	0.266	0.245
OCR21	100/1	50	50	0.4	0.8

Table 9
Tripping times for primary and backup OCR pairs during faults.

Fault Current	OCR	Fault Current	Tripping Time (s)	
			Standard	Non-standard
F1	OCR 1	630	0.022	0.022
	OCR 2	630	0.306	0.305
F2	OCR 2	963	0.306	0.23
	OCR 3	963	0.59	0.53
F3	OCR 3	1382	0.59	0.38
	OCR 4	1382	0.90	0.68
F4	OCR 4	1501	0.90	0.65
	OCR 5	1501	1.21	0.96
F5	OCR 5	1901	1.21	0.83
	OCR 6	1453	1.5	1.13
F6	OCR 6	2771	1.45	0.80
	OCR 7	2771	1.75	1.11
F7	OCR 7	4392	1.75	0.79
	OCR 8	4392	2.06	1.11
F8	OCR 8	5727	2.06	0.86
	OCR9	5727	2.31	1.16
F9	OCR9	8082	2.31	0.72
	OCR10	8082	2.61	1.02
F10	OCR10	17913	2.61	0.47
	OCR11	17913	2.92	0.77
F11	OCR12	845	0.13	0.11
	OCR13	845	0.43	0.41
F12	OCR13	1350	0.43	0.33
	OCR14	1350	0.73	0.63
F13	OCR14	1916	0.73	0.51
	OCR15	1916	1.02	0.81
F14	OCR16	2204	0.022	0.01
	OCR17	2204	0.302	0.302
F15	OCR18	1976	0.022	0.008
	OCR19	1976	0.306	0.304
F16	OCR19	3562	0.30	0.001
	OCR20	3562	0.60	0.304
F17	OCR20	5970	0.60	0.13
	OCR21	5970	0.90	0.43

Table 10
Overall tripping time for OCRs.

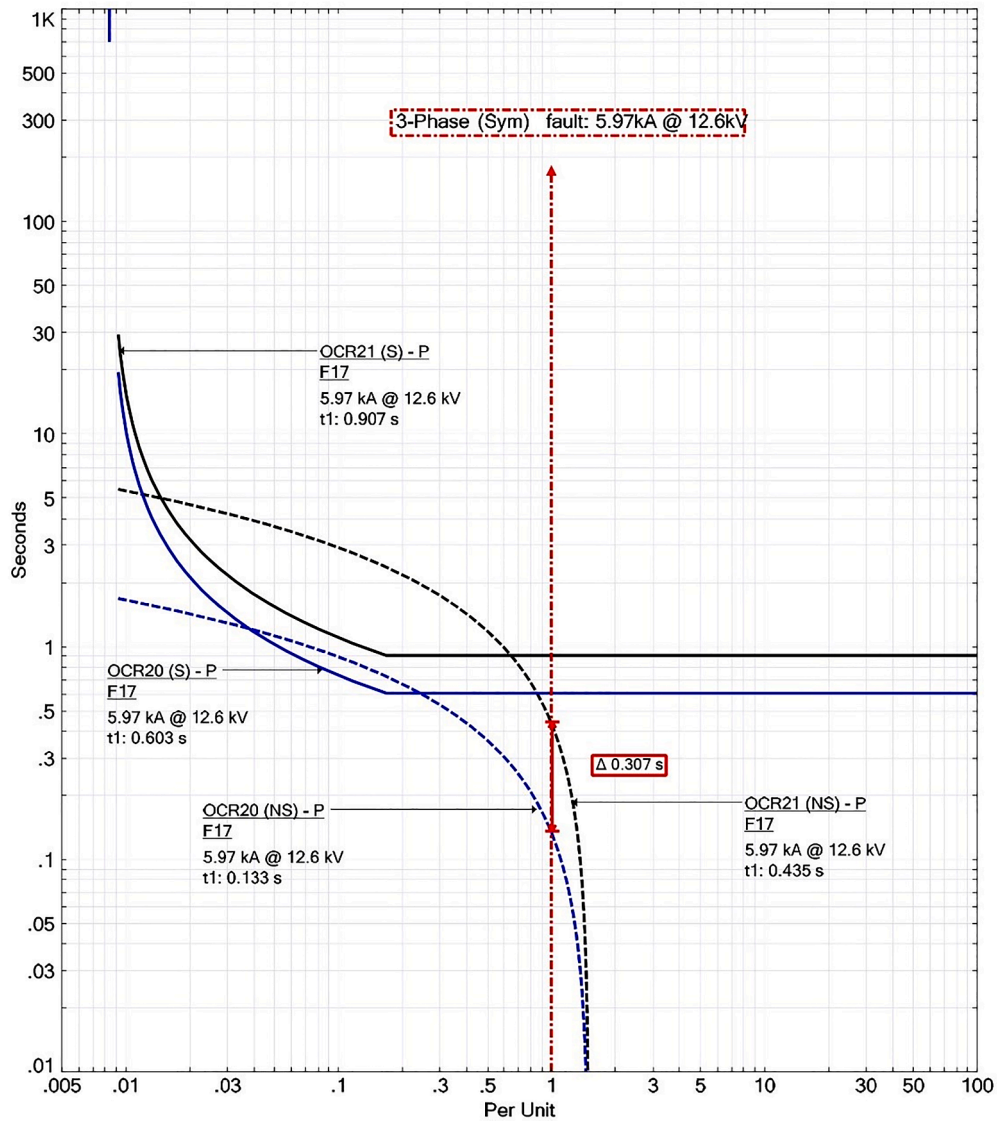| Protection scheme	Overall operation time (Seconds)
Standard scheme	35.896
Non-standard scheme	18.816

Fig. 20. The coordination between primary and secondary OCRs.

Declaration of competing interest

No conflict of interest.

Data availability

Derived data supporting the findings of this study are available from the corresponding author on request.

Acknowledgement

References

[1] Gadanayak DA. Protection algorithms of microgrids with inverter interfaced distributed generation units—a review. Electr Power Syst Res 2021;192:106986.
[2] Sultan V, Hilton B. Electric grid reliability research. Energy Inform 2019;2(1).
[3] Singh SRK, Chaturvedi SIS, Kumar SA, Kumar SA, Patwardhan VA, Jagdale DD, Sinha SAK, Yadav SBP. Ministry of new and renewable energy (MNRE). Water Energy Int 2020;63(8):6–8.
[4] Alasali F, Itradat A, Abu Ghalyon S, Abudayyeh M, El-Naily N, Hayajneh AM, AlMajali A. Smart grid resilience for grid-connected PV and protection systems under cyber threats. Smart Cities 2024;7:51–77.
[5] Choi J, Debnath S. Electromagnetic transient (EMT) simulation algorithm for evaluation of photovoltaic (PV) generation systems. In: 2021 IEEE Kansas Power and Energy Conference (KPEC); 2021. p. 1–6.
[6] Ekic A, Strombeck B, Wu D, Ji G. Assessment of grid strength considering interactions between inverter-based resources and shunt capacitors. In: 2020 IEEE Power & Energy Society General Meeting (PESGM); 2020. p. 1–5.
[7] Resource, M.F.I.S.P.. 1,200 mw fault induced solar photovoltaic resource interruption disturbance report: Southern California 8/16/2016 event. Atlanta, GA: NERC; 2017. https://www.nerc.com/pa/rrm/ea/1200_MW_Fault_Induced_Solar_Photovoltaic_Resource_/1200_MW_Fault_Induced_Solar_Photovoltaic_Resource_Interruption_Final.pdf. Date accessed 30 March 2024.
[8] NERC W, et al. 900 mw fault induced solar photovoltaic resource interruption disturbance report. North American Electric Reliability Corporation; 2018. https://www.nerc.com/pa/rrm/ea/October%209%202017%20Canyon%202%20Fire%20Disturbance%20Report/900%20MW%20Solar%20Photovoltaic%20Resource%20Interruption%20Disturbance%20Report.pdf. Date accessed 30 March 2024.
[9] NERC W. April and May 2018 fault induced solar photovoltaic resource interruption disturbance report. North American Electric Reliability Corporation; 2019. https://www.nerc.com/pa/rrm/ea/April_May_2018_Fault_Induced_Solar_PV_Resource_Int/April_May_2018_Solar_PV_Disturbance_Report.pdf. Date accessed 30 March 2024.
[10] Memon AA, Kauhaniemi K. A critical review of ac microgrid protection issues and available solutions. Electr Power Syst Res 2015;129:23–31.
[11] Gers JM, Holmes EJ. Protection of electricity distribution networks. IET Power Energy Ser 2004;47:47. 2nd Edition.
[12] Mansour MM, Mekhamer SF, El-Kharbawe N. A modified particle swarm optimizer for the coordination of directional overcurrent relays. IEEE Trans Power Deliv 2007;22(3):1400–10.
[13] Mohammadi R, Abyaneh H, Razavi F, Al-Dabbagh M, Sadeghi S. Optimal relays coordination efficient method in interconnected power systems. J Electr Eng 2010;61(2):75.
[14] Rivas AEL, Pareja LAG, Abrao T. Coordination of distance and directional overcurrent relays using an extended continuous domain ACO algorithm and an hybrid ACO algorithm. Electr Power Syst Res 2019;170:259–72.
[15] Najy WK, Zeineldin HH, Woon WL. Optimal protection coordination for microgrids with grid-connected and islanded capability. IEEE Trans Ind Electr 2012;60 (4):1668–77.
[16] Srinivas S, Verma PP, Swarup KS. A novel convexified linear program for coordination of directional overcurrent relays. IEEE Trans Power Deliv 2019;34(2): 769–72.
[17] Urdaneta AJ, Nadira R, Jimenez LP. Optimal coordination of directional overcurrent relays in interconnected power systems. IEEE Trans Power Deliv 1988;3(3): 903–11.
[18] Alam MN. Overcurrent protection of ac microgrids using mixed characteristic curves of relays. Comput Electr Eng 2019;74:74–88.
[19] Bedekar PP, Bhide SR. Optimum coordination of directional overcurrent relays using the hybrid GA-NLP approach. IEEE Trans Power Deliv 2010;26(1):109–19.
[20] Sharaf HM, Zeineldin H, Ibrahim DK, Essam E. A proposed coordination strategy for meshed distribution systems with dg considering user-defined characteristics of directional inverse time overcurrent relays. Int J Electr Power Energy Syst 2015;65:49–58.
[21] Biswal S, Samantaray S. A user defined characteristics based optimal coordination of directional overcurrent relay for microgrids. In: 2021 National Power Electronics Conference (NPEC); 2021. p. 01–6.
[22] Salazar CAC, Enríquez AC, Schaeffer SE. Directional overcurrent relay coordination considering non-standardized time curves. Electr Power Syst Res 2015;122: 42–9.
[23] Ezzeddine M, Kaczmarek R, Iftikhar M. Coordination of directional over- current relays using a novel method to select their settings. IET Generat Transmiss Distrib 2011;5(7):743–50.
[24] Yazdaninejadi A, Golshannavaz S, Nazarpour D, Teimourzadeh S, Aminifar F. Dual-setting directional overcurrent relays for protecting automated distribution networks. IEEE Trans Industr Inform 2018;15(2):730–40.
[25] Keil T, Jager J. Advanced coordination method for overcurrent protection relays using nonstandard tripping characteristics. IEEE Trans Power Deliv 2008;23(1): 52–7.
[26] Papaspiliotopoulos VA, Korres GN, Kleftakis VA, Hatziargyriou ND. Hardware-in-the-loop design and optimal setting of adaptive protection schemes for distribution systems with distributed generation. IEEE Trans Power Deliv 2015;32(1):393–400.
[27] Muda H, Jena P. Sequence currents based adaptive protection approach for distribution networks with distributed energy resources. IET Generat Transmiss Distrib 2017;11(1).
[28] El-Naily N, Saad SM, Hussein T, Mohamed FA. A novel constraint and non-standard characteristics for optimal over-current relays coordination to enhance microgrid protection scheme. IET Generat Transmiss Distrib 2018;13(6):780–93.
[29] Fani B, Bisheh H, Sadeghkhani I. Protection coordination scheme for distribution networks with high penetration of photovoltaic generators. IET Generat Transmiss Distrib 2018;12(8):1802–14.
[30] Mahindara VR, Rodriguez DFC, Pujiantara M, Priyadi A, Purnomo MH, Muljadi E. Practical challenges of inverse and definite-time overcurrent protection coordination in modern industrial and commercial power distribution system. IEEE Trans Ind Appl 2020;57(1):187–97.
[31] Sorrentino E, Rodríguez JV. Effects of the curve type of overcurrent functions and the location of analyzed faults on the optimal coordination of directional overcurrent protections. Comput Electr Eng 2020;88:106864.
[32] Yazdaninejadi A, Golshannavaz S. Robust protection for active distribution networks with islanding capability: An innovative and simple cost-effective logic for increasing fault currents virtually. Int J Electr Power Energy Syst 2020;118:105773.
[33] Darabi A, Bagheri M, Gharehpetian G. Highly sensitive microgrid protection using overcurrent relays with a novel relay characteristic. IET Renew Power Gener 2020;14(7):1201–9.
[34] Alasali F, El-Naily N, Zarour E, Saad SM. Highly sensitive and fast micro- grid protection using optimal coordination scheme and nonstandard tripping characteristics. Int J Electr Power Energy Syst 2021;128:106756.
[35] Narimani A, Hashemi-Dezaki H. Optimal stability-oriented protection coordination of smart grid's directional overcurrent relays based on optimized tripping characteristics in double-inverse model using high-set relay. Int J Electr Power Energy Syst 2021;133:107249.
[36] Wong JYR, Tan C, Che HS, et al. Selectivity problem in adaptive overcurrent protection for microgrid with inverter-based distributed generators (IBDG): theoretical investigation and HIL verification. IEEE Trans Power Deliv 2021;37(4):3313–24.
[37] Barra PHA, Lacerda V, Fernandes R, Coury DV. A hardware-in-the-loop testbed for microgrid protection considering non-standard curves. Electr Power Syst Res 2021;196:107242.

[38] Abeid S, Hu Y, Alasali F, El-Naily N. Innovative optimal nonstandard trip- ping protection scheme for radial and meshed microgrid systems. Energies (Basel) 2022;15(14):4980.

[39] Ataee-Kachoee AH, Hashemi-Dezaki H, Ketabi A. Optimal adaptive protection of smart grids using high-set relays and smart selection of relay tripping characteristics considering different network configurations and operation modes. IET Generat Transmiss Distrib 2022;16(24):5084–116.

[40] Tripathi JM, Mallik SK. An adaptive protection coordination strategy utilizing user-defined characteristics of DOCRs in a microgrid. Electr Power Syst Res 2023; 214:108900.

[41] Zand HK, Mazlumi K, Bagheri A, Hashemi-Dezaki H. Optimal protection scheme for enhancing ac microgrids stability against cascading outages by utilizing events scale reduction technique and fuzzy zero-violation clustering algorithm. Sustainability 2023;15(21):15550.

[42] Rizwan M, Gao C, Yan X, Ahmad S, Zaindin M. An approach to disparage the blindness of backup protection in grid connected renewable energy sources system by inducing artificial fault current. Int J Electr Power Energy Syst 2023;153:109185.

[43] Sati TE, Azzouz MA, Shaaban MF. Adaptive harmonic-based protection coordination for inverter-dominated isolated microgrids considering n-1 contingency. Int J Electr Power Energy Syst 2024;156:109750.

[44] Tjahjono A, Anggriawan DO, Faizin AK, Priyadi A, Pujiantara M, Taufik T, Purnomo MH. Adaptive modified firefly algorithm for optimal coordination of overcurrent relays. IET Generat Transmiss Distrib 2017;11(10):2575–85.

[45] Saldarriaga-Zuluaga SD, Lòpez-Lezama JM, Muñoz-Galeano N. Optimal coordination of overcurrent relays in microgrids considering a non-standard characteristic. Energies (Basel) 2020;13(4):922.

[46] El-Naily N, Saad SM, Mohamed FA. Novel approach for optimum coordination of overcurrent relays to enhance microgrid earth fault protection scheme. Sustain Cities Soc 2020;54:102006.

[47] Alasali F, El-Naily N, Zarour E, Saad S. Highly sensitive and fast microgrid protection using optimal coordination scheme and nonstandard tripping characteristics. Int J Electr Power Energy Syst 2021;128:106756.

[48] Alasali F, Zarour E, Holderbaum W, Nusair K. Highly fast innovative overcurrent protection scheme for microgrid using metaheuristic optimization algorithms and nonstandard tripping characteristics. IEEE Access 2022;10:42208.

[49] Sadollah A, Eskandar H, Kim J. Water cycle algorithm for solving constrained multi-objective optimization problems. Appl Soft Comput 2015;27.

[50] Coleman T, Branch M, Grace A. Optimization Toolbox, For Use with MATLAB. User's Guide for MATLAB 5; Version 2; Relaese II. Natica, MA, USA: The MathWorks Inc.; 1990.